

Mu2e-II: Searching for Muon-to-Electron Conversion in the PIP-II Era

Presented by Sophie Middleton

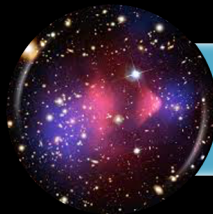
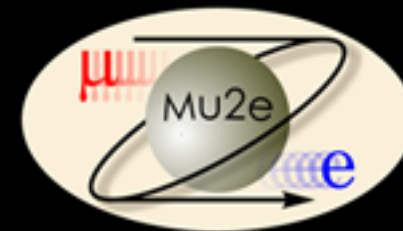
24 – 27th May 2021

Workshop on Potential Muon Campus at Fermilab and Storage Ring Experiments

Outline



Charged Lepton Flavor Violation (CLFV)



Physics Reach & Other Channels



The Mu2e Experiment: Current Status



The Mu2e-II Experiment



Summary

Introduction

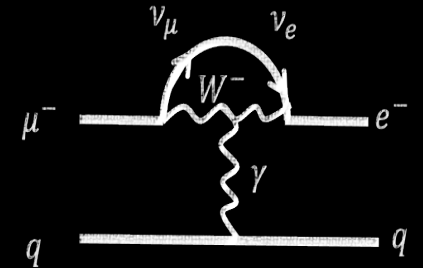
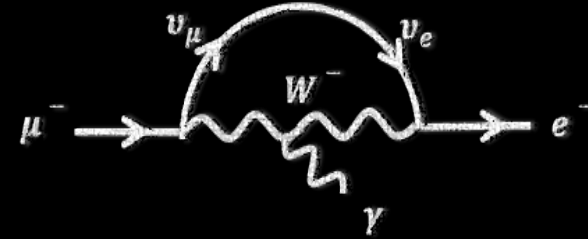
Charged Lepton Flavor Violation (CLFV)

- The minimal extension of the Standard Model, including Dirac masses of neutrinos, allows for CLFV at loop level, mediated by W bosons.
- However, rates are heavily suppressed by GIM suppression and are far below any conceivable experiment could measure, for example:

$$B(\mu \rightarrow e\gamma) = \frac{3\alpha}{32\pi} \left| \sum_{i=2,3} U_{\mu i}^* U_{ei} \frac{\Delta m_{1i}^2}{M_W^2} \right|^2 \quad [1-4]$$

$$B(\mu \rightarrow e\gamma) = \frac{3\alpha}{32\pi} \left(\frac{1}{4} \right) \sin^2 2\theta_{13} \sin^2 \theta_{23} \left| \frac{\Delta m_{13}^2}{M_W^2} \right|^2$$

$$B(\mu \rightarrow e\gamma) \approx \mathcal{O}(10^{-54})$$

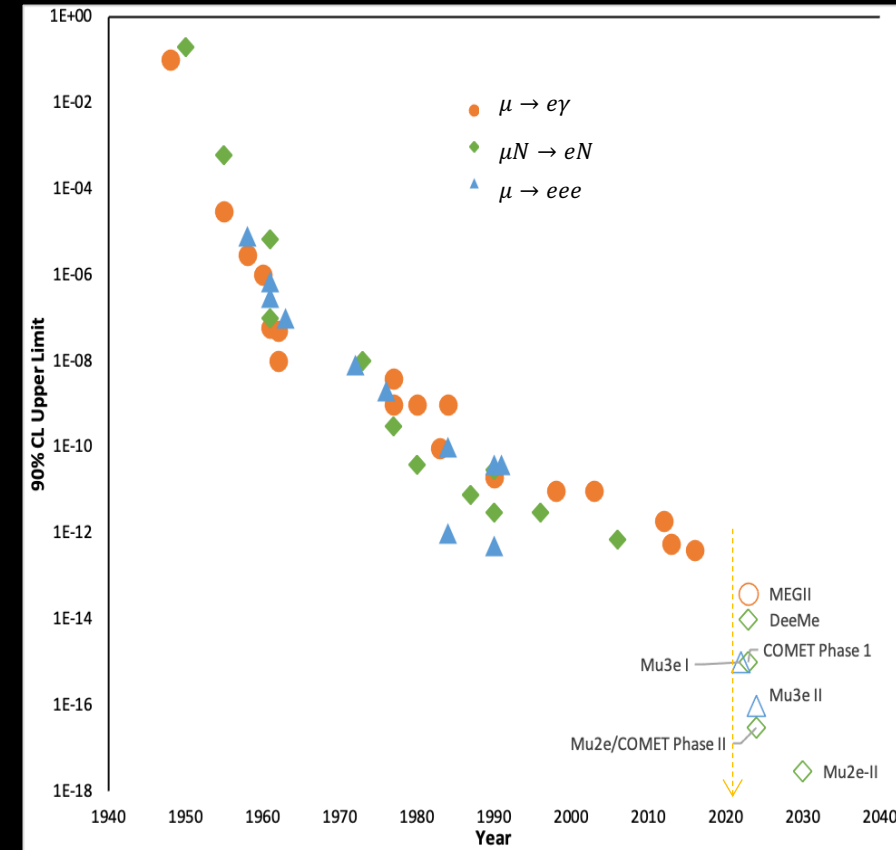


- using best-fit values for neutrino data ($m_{\nu j}$ for the neutrino mass and U_{ij} for the element of the PMNS matrix).
- Mu2e/Mu2e-II will search for the coherent, neutrinoless conversion of the muon to the electron in the presence of a nucleus.
- If observed, this would be an unambiguous sign of physics beyond the Standard Model (BSM).

Experimental Searches for CLFV

- $\mu^- N \rightarrow e^- N$ searches are crucial part of global program searching for CLFV.
- Muons offer more powerful probe for CLFV compared to taus.
- To elucidate the mechanism responsible for any CLFV – must look at relative rates (if any) in different muon channels.

Mode	Current Limit (at 90% CL)	Future Proposed Limit	Future Experiment/s
$\mu^\pm \rightarrow e^\pm \gamma$	4.2×10^{-13} [5]	4×10^{-14}	MEG II [8]
$\mu^- N \rightarrow e^- N$	7×10^{-13} [6]	10^{-15} 10^{-17} 10^{-18}	COMET Phase-I Mu2e [10] & COMET Phase-II [9] Mu2e-II
$\mu^+ \rightarrow e^+ e^+ e^-$	$\sim 10^{-12}$ [7]	$10^{-15} \sim 10^{-16}$	Mu3e



$$R_{\mu e} = \frac{\Gamma(\mu^- + A(Z, N) \rightarrow e^- + A(Z, N))}{\Gamma(\text{all-captures})} < 7 \times 10^{-13} (90\% \text{C.L.})$$

- Muon-to-electron sector provides powerful probes and complements collider searches for $\tau \rightarrow e\gamma$ or $\mu\gamma$ and $H \rightarrow e\tau$, $\mu\tau$, or μe .

Simplistic Explanation of Physics Reach

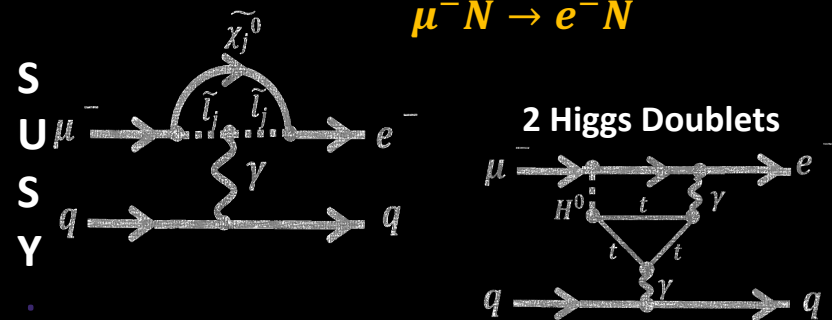
Mu2e & Mu2e-II can probe very high mass scales $O(1000 - 10,000 \text{ TeV})$

A. de Gouvêa, P. Vogel
arXiv:1303.4097

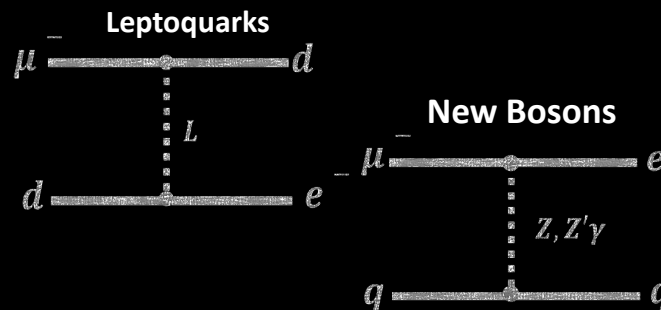
- For the purposes of discussion we can build a Toy Lagrangian which consists of 2 terms representing 2 types of physics process:

$$\mathcal{L}_{CLFV} = \frac{m_\mu}{(1+\kappa)\Lambda^2} \bar{\mu}_R \sigma_{\mu\nu} e_L F^{\mu\nu} + \frac{\kappa}{(1+\kappa)\Lambda^2} \bar{\mu}_L \gamma_\mu e_L \left(\sum_{q=u,d} \bar{q}_L \gamma_\mu q_L \right)$$

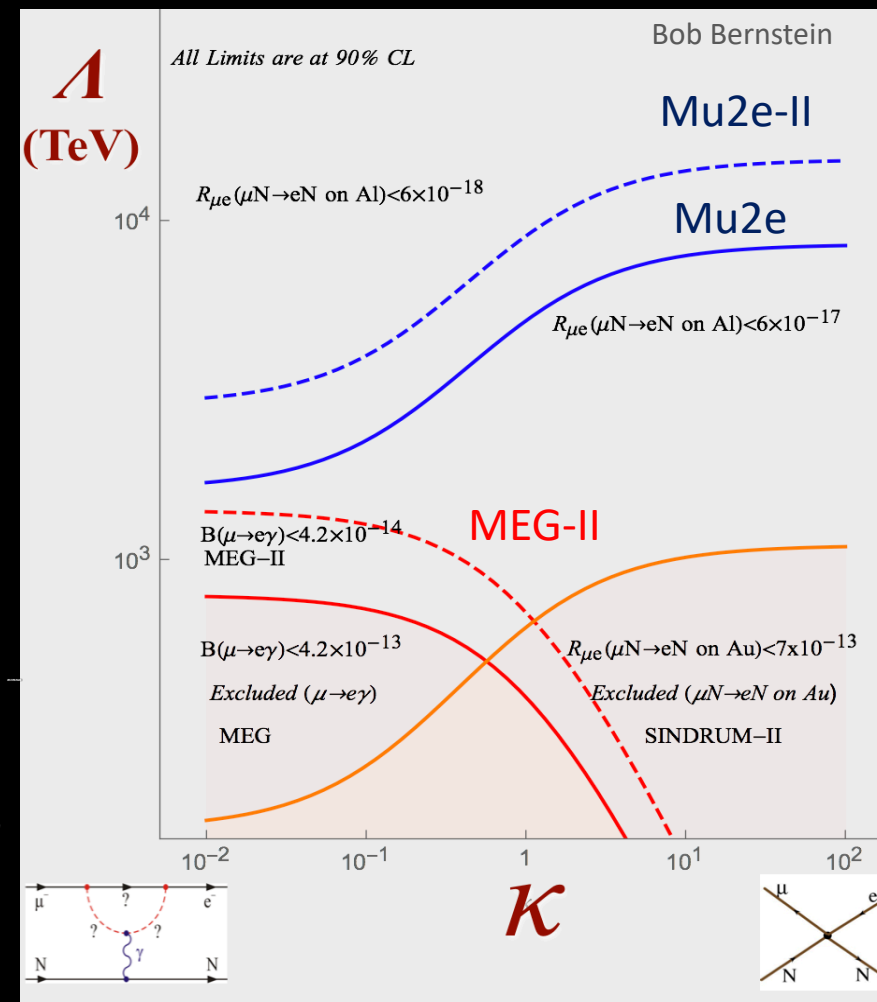
“Photonic”
i.e. Dipole terms:
 $\mu^\pm \rightarrow e^\pm \gamma$, $\mu \rightarrow eee$
 $\mu^- N \rightarrow e^- N$



“Contact”
i.e. 4 fermion terms
Only $\mu^+ \rightarrow e^+ e^+ e^-$
And $\mu^- N \rightarrow e^- N$



Λ : effective mass scale of New Physics (NP),
 κ : determines to what extent NP is photonic ($\kappa \ll 1$) or 4-fermion ($\kappa \gg 1$)



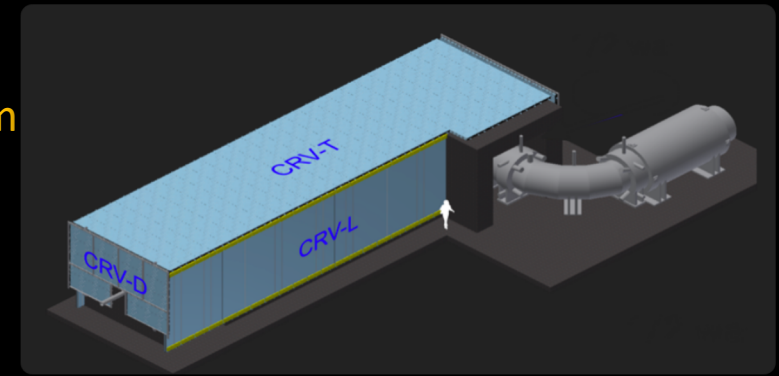
Mu2e: Status & Timeline

Mu2e: Design

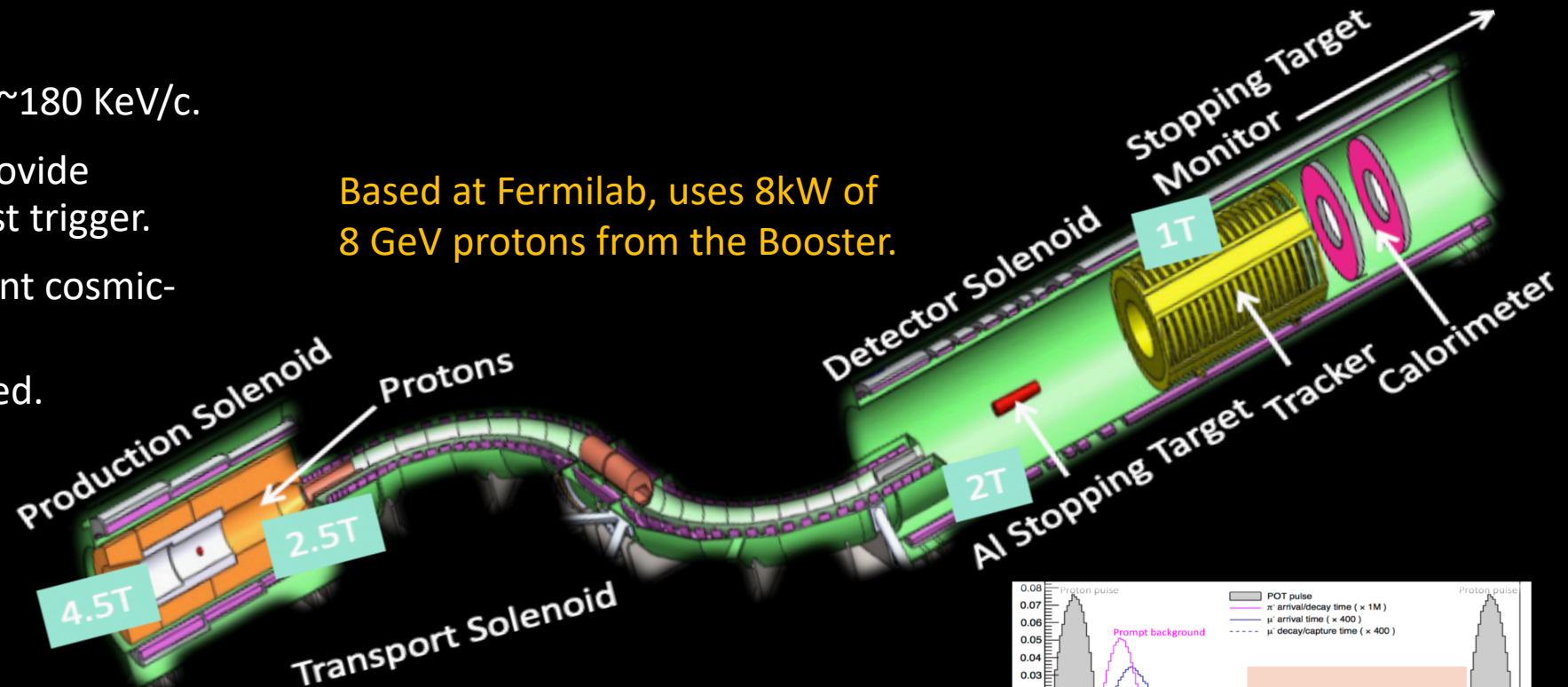
- 3 Superconducting Solenoid Systems:
 - Production, Transport and Detector
 - Graded magnetic field.
- Low mass annular straw tube tracker:
 - > 20,000 straws;
 - wall thickness 15 μm ;
 - provides momentum resolution $\sim 180 \text{ KeV/c}$.
- 1348 CsI crystals in 2 annular rings provide complementary information and a fast trigger.
- Cosmic-Ray Veto (CRV) detects incident cosmic-ray muons.
 - Veto efficiency of 99.99% required.

Based on MELC: V. Lobashev & R. Djilkibaev (Sov. J. Nucl. Phys. 49(2), 384 (1989))

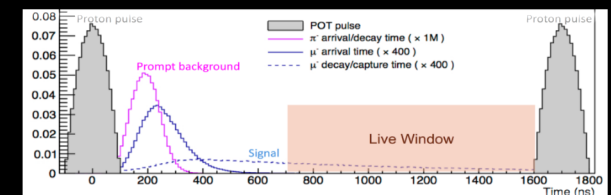
Active Cosmic Ray Veto System
surrounds the Detector
Solenoid



25 m in total



Based at Fermilab, uses 8kW of
8 GeV protons from the Booster.



Mu2e-II: A Muon-to-Electron Search in the PIP-II Era - Sophie Middleton -
smidd@caltech.edu

Transport Solenoid at Fermilab



Shield shown next to TSu



TS coldmass at Fermilab awaiting final tests.



Warm bore and thermal shield procurement completed

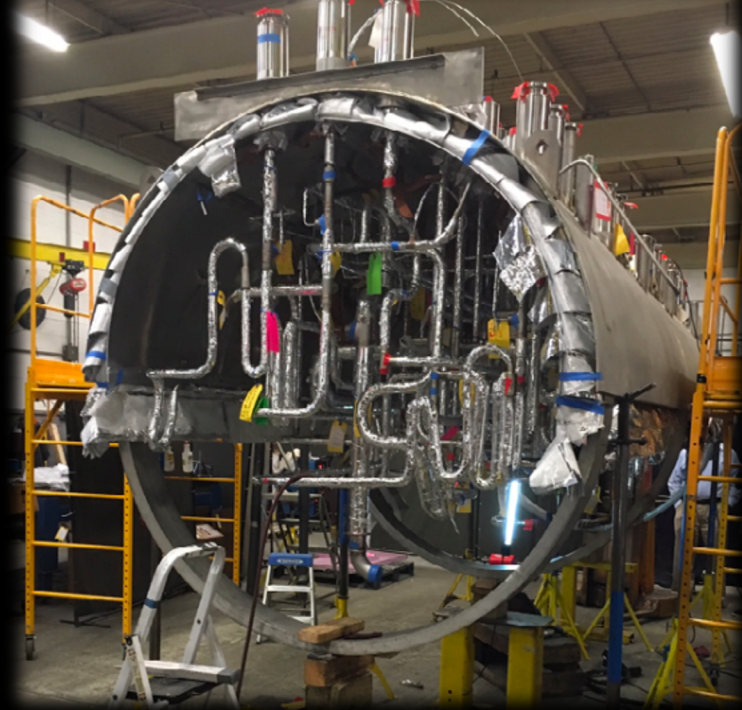
- All coils of the TS are now at Fermilab
- Final tests ongoing throughout past year
- Outer thermal shield will be split and re-assembled around the TSu coldmass alongside

Both TSu and TSd are at FNAL



PS & DS Progress

Cryogenic Distribution Box at Fermilab



Production Target Fabricated



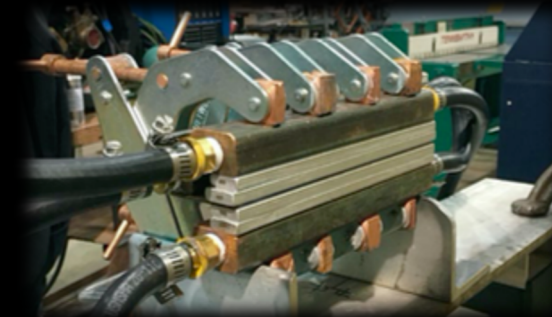
Example PS coil



Production Target Frame



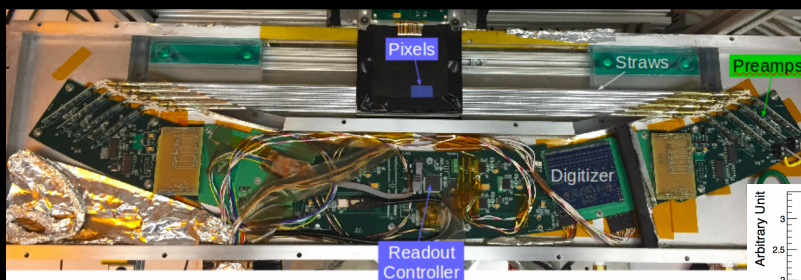
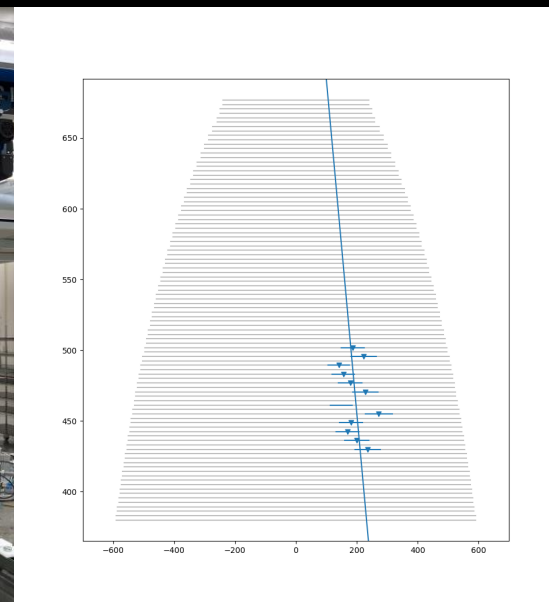
Splice Validation



Heat & Radiation Shield

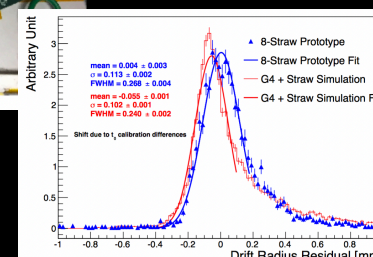
The Tracker: Progress

2020: Production at University of Minnesota, testing at Duke Uni., shipping to FNAL.



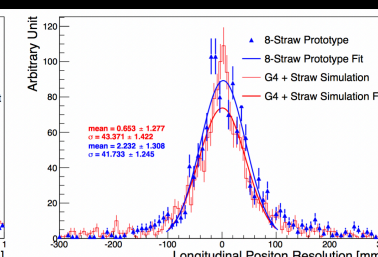
2018: Prototype at Berkeley/LBNL

Prototype measured performance and resolutions.
→ Meet requirements!



Transverse Resolution
(Data vs MC)

$$\sigma_{data} = 0.113 \pm 0.002 \text{ mm}$$
$$\sigma_{MC} = 0.102 \pm 0.001 \text{ mm}$$



Longitudinal Resolution
(Data vs MC)

$$\sigma_{data} = 42 \pm 1 \text{ mm}$$
$$\sigma_{MC} = 43 \pm 1 \text{ mm}$$

Calorimeter: Progress

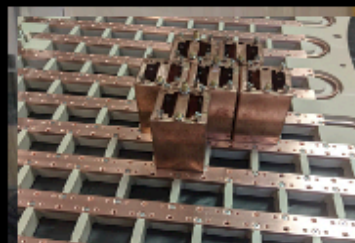
**2021: Begin
calorimeter frame
assembly at FNAL**



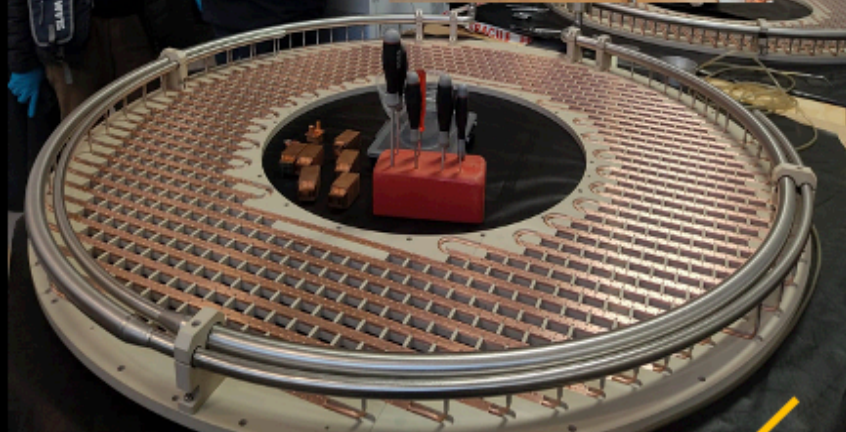
Inner Ring



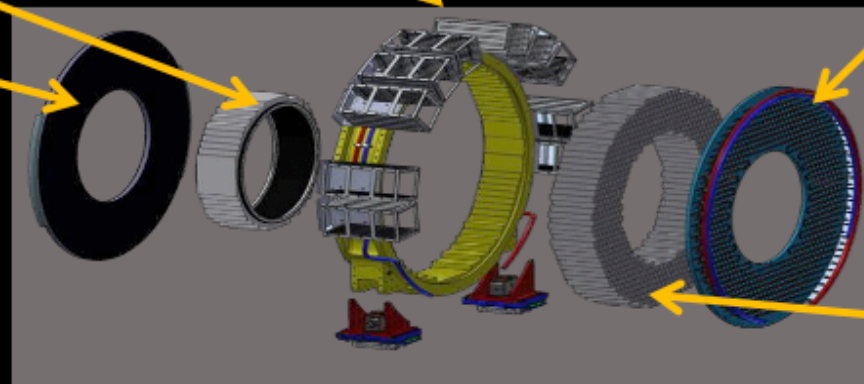
Outer ring at FNAL



SiPMs glued into boards



FEE Board



**CsI crystals at
FNAL in sealed
cupboard after
QA.**



Source Calibration System

Caltech

Mu2e: Current Status

- Mu2e construction is nearly complete:
 - Beamline is finished.
 - Superconducting cable for all solenoids procured, winding for all three solenoid units is well-underway.
 - Transport Solenoid coils arrived at Fermilab, final testing and assembly underway.
 - Tracker straws, FEE prototypes, calorimeter crystals and SiPMs, STM detectors, and CRV counters are complete.
 - Assembly and testing of these detector components is on-going.
- Transition to installation in 2021;
- Detector Cosmic Ray Commissioning 2022;
- Commissioning with beam continuing 2023;
- Physics running is expected 2024.

Mu2e-II

Motivations

Mu2e-II aims to improve the sensitivity ($R_{\mu e}$) to the neutrinoless conversion of a muon-to an-electron in the field of a nucleus by a further order of magnitude than Mu2e i.e. $SES \sim \mathcal{O}(10^{-18})$

- There are 2 possible outcomes from Mu2e:
 1. **Conversion not observed** - motivates pushing to higher mass scales .
 2. **Conversion observed** - motivates more precise measurements with different targets.
- Either way Mu2e-II is well motivated!

Mu2e-II would:

- Be based at Fermilab. Will utilize the (nominal) 100kW beam from Proton Improvement Plan II (PIP-II).
- Start a few years after the end of Mu2e run with an expected 3+1 years of physics running.
- Salvage and refurbish as much of Mu2e infrastructure as possible.
- Upgrade Mu2e components where required to handle higher beam intensity.

The PIP-II Project

- The project received CD-1 approval from the U.S. Department of Energy in July 2018.
- PIP-II will power both DUNE and other experiments like Mu2e-II.
- PIP-II is planned to deliver beam in the next decade.
- Groundbreaking ceremony took place in 2019.

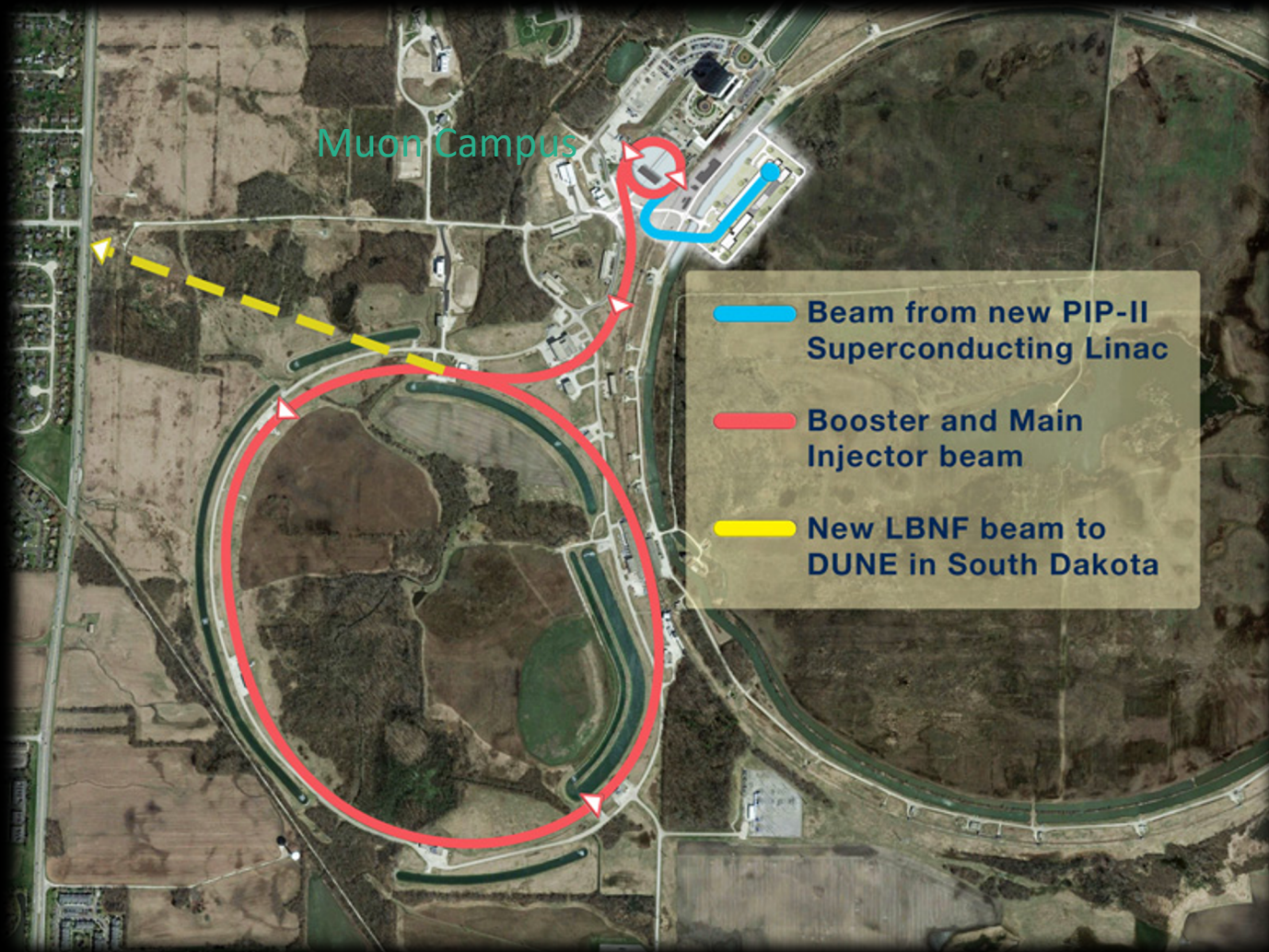


2021



2025

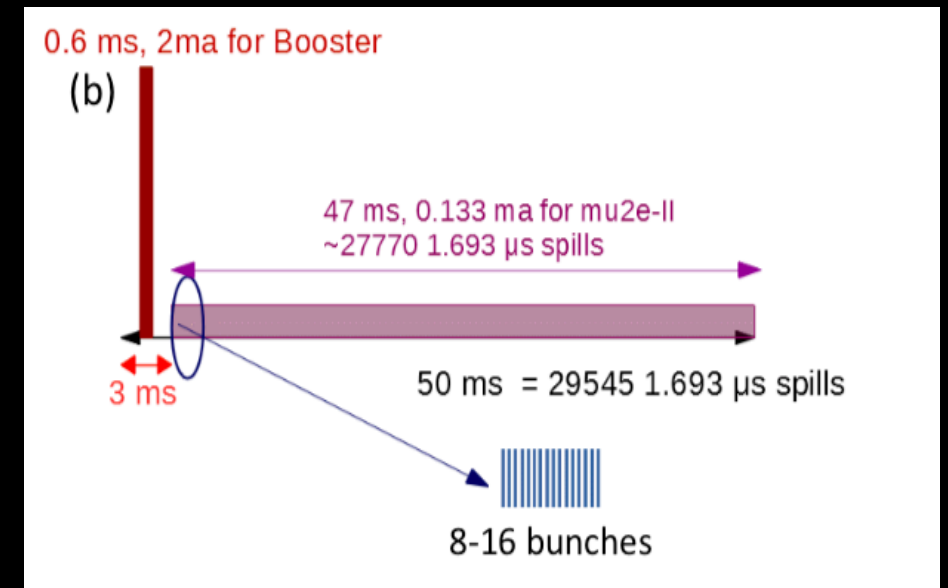
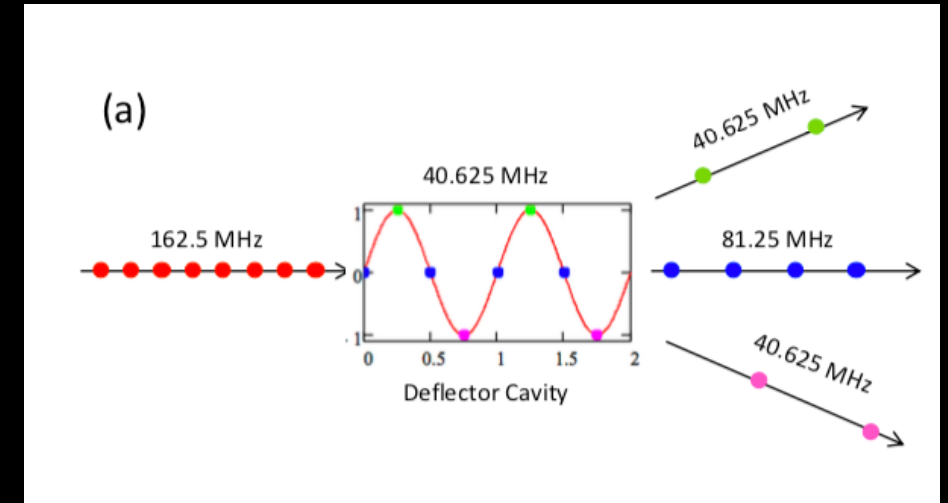
PIP-II



- PIP-II designed to deliver 800 MeV H⁻ beam to the Booster.
- Capable of running in CW mode with 2 mA average current at 1.6 MW .
- Mu2e-II will get a beam at upstream end of transfer line to Booster:
 - Need to build a beamline to deliver beam to M4 enclosure

Mu2e-II Beam Delivery

- The high energy program will use ~1% of the available beam pulses.
- Leading concept for remaining beam involves a 40.625 MHz RF deflector to split the beam into three sub-lines.
- Assume Mu2e-II will have access to the central (node) line, and will be able to receive bunches at up to 81.25 MHz.
- In Mu2e-II:
 - 8 bunches of 2×10^8 each,
 - pulses 1700 ns apart
 - 118 kW at 800 MeV > order of magnitude increase on Mu2e
- Most of the R&D effort for all subsystems comes from understanding how to cope with this increased intensity.

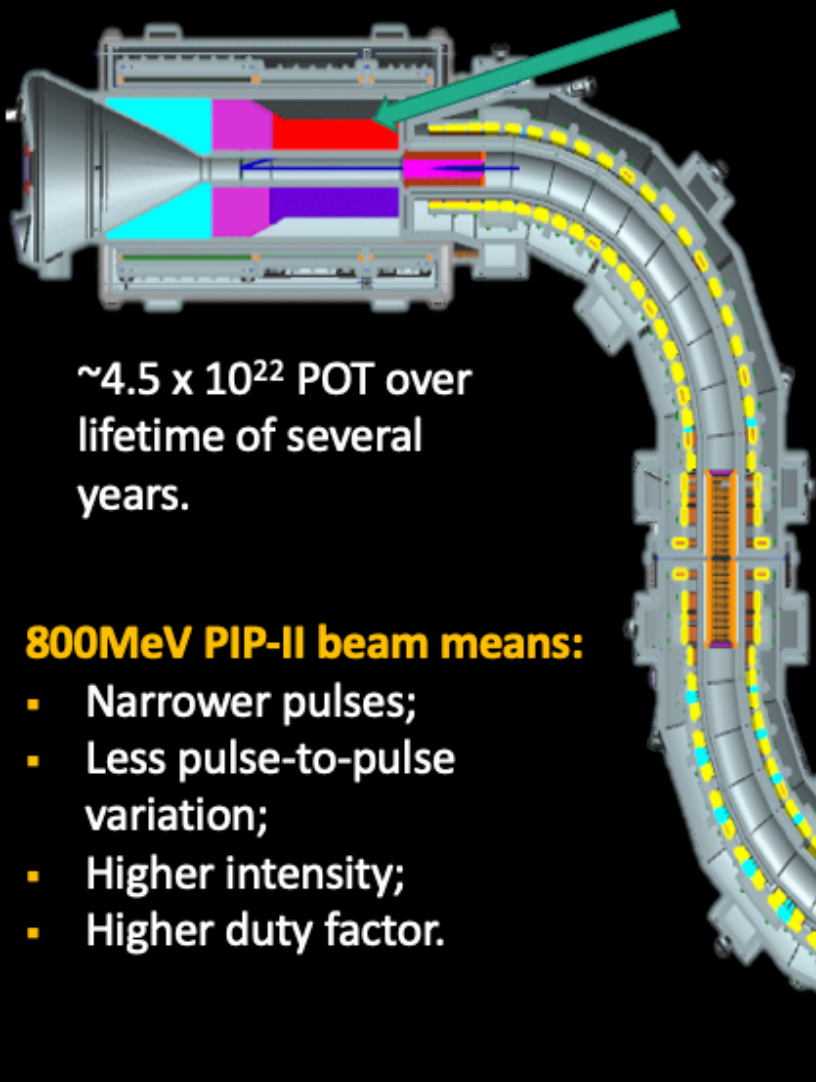


Beam Requirements

- PIP-II can deliver these requirements to Mu2e-II

	Mu2e	Mu2e-II	comments
Source	Slow extracted from Delivery Ring	H- direct from PIP-II Linac	Mu2e-II will need to strip H- ions upstream of the production target
Beam energy [MeV]	8000	800	Optimal beam energy 1-3 GeV
Total POT	3.6×10^{20}	4.5×10^{22}	Approx.
Lifetime [yr]	3	3	
Run Time [sec/yr]	2×10^7	2×10^7	
Duty factor	25%	>90%	Important for keeping instantaneous rates under control
P pulse width [ns]	250	100	
P pulse spacing [ns]	1695	1700	Assumes Al target
Extinction	1×10^{-10}	1×10^{-11}	Ratio of out:in time protons
Average beam power [kW]	8	100	100kW approx.

Mu2e-II Beam



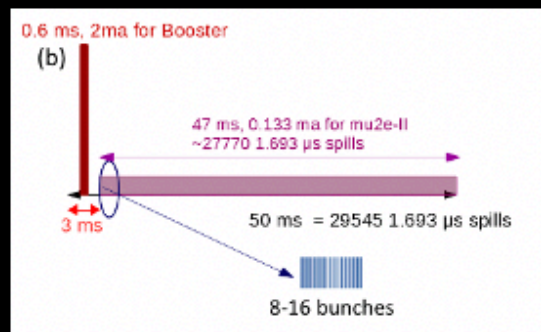
$\sim 4.5 \times 10^{22}$ POT over lifetime of several years.

800MeV PIP-II beam means:

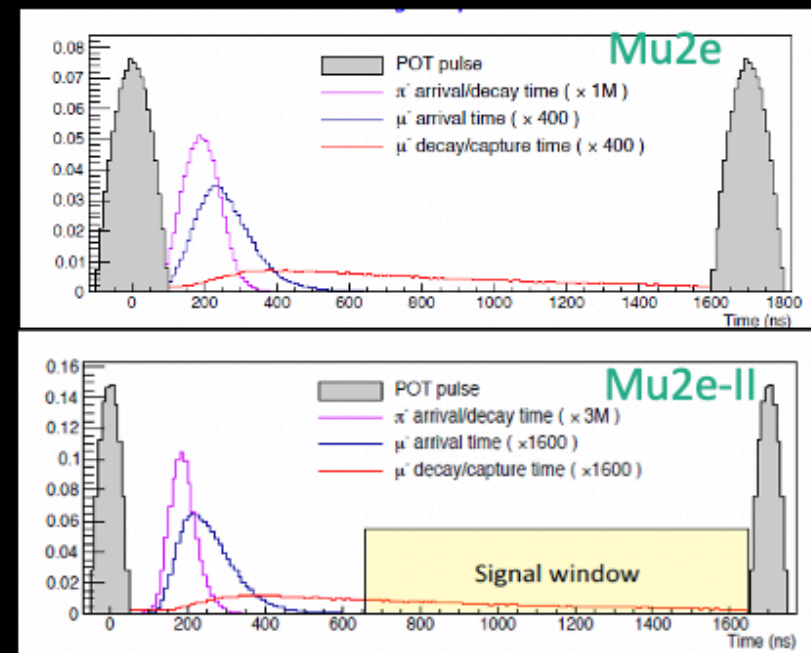
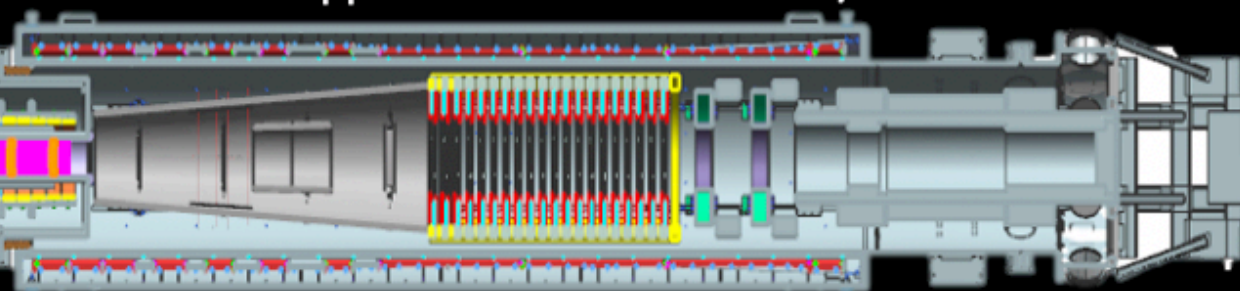
- Narrower pulses;
- Less pulse-to-pulse variation;
- Higher intensity;
- Higher duty factor.

Mu2e-II will have similar design to Mu2e:

1. 3 solenoids: PS, TS, DS
2. Removed Anti-proton Windows
3. Redesign detectors for intense rate



Estimated Stopped Muon rate = 0.00009/POT



Required Changes in Beam Delivery

Changing beam energy and increasing the power present a number of challenges:

- **Magnetic Stripping:** High fields in the PS strip out electron before the particles hit the target
→ *Include a stripping foil in beam transport and design for the beam loss that it would produce.*
- **Production:** PS field perturbs 800 MeV beam more. Existing beam injection port and target orientation will not work. HRS will intersect beam path and will not provide shielding from higher beam intensity.
→ *HRS redesign. Significant modification to, or replacement of, the Production Solenoid.*
- **Beam Power and Beam Dump:** Target must be re-redesigned for the increased beam power. The lower beam energy means that the beam that goes through the target will not be correctly targeted at the beam dump.
- **Extinction:** Mu2e-II will need x10 more extinction. Extinction of beam out of the linac is only guaranteed to be 10^{-4} , so active extinction system will have to provide 10^{-9} extinction.
- **Extinction Monitor:** Entrance collimator of the spectrometer will not be aligned correctly for the lower energy particles produced by the 800 MeV beam.
→ *Reworking the extinction monitor requires R&D and effort.*

Apparatus

Production Target

LDRD Project on-going to investigate production target choice

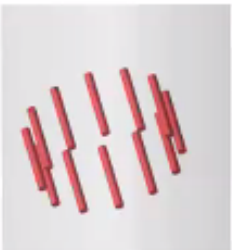
	Tungsten/WC	Lower-density bent (Carbon)
Rotated	Requires a large hardware in HRS	Too large to fit HRS
Fixed granular	DPA is too high	DPA is high; lower pion production
Conveyor	Thermal analysis is ongoing	Lower pion production; thermal analysis is ongoing

Front runner is Conveyor design. But made out of W or C?

Prioritizing designs

- Constraint: compatibility with the current HRS design (inner bore=20 (25) cm)

Rotator



Pros: radiation damage can be distributed over many rods
Cons: its hardware would require a significant space inside the bore (complicates cooling and muon flow)

Granular

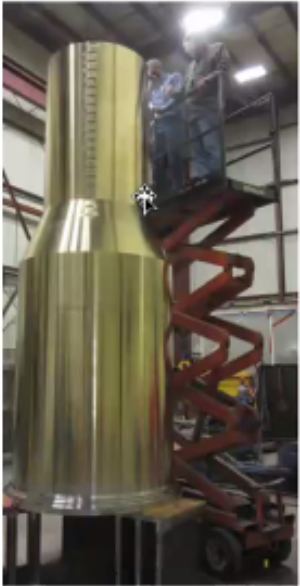


Pros: small space required
Cons: peak DPA (MARS15) >300/yr; gas cooling cannot be performed efficiently

Conveyor



Pros: small space required; He gas could be used for both cooling and moving elements inside conveyor; radiation damage can be distributed; **Cons:** technical complexity (prototyping needed)



(blofoylbiu8 ueeqeq)
tecni9aj cowaibexil
qisupnre9: **cons:**
qaw98e csu p6
coulelou: u9qis9iou

Muon Stopping Target Materials

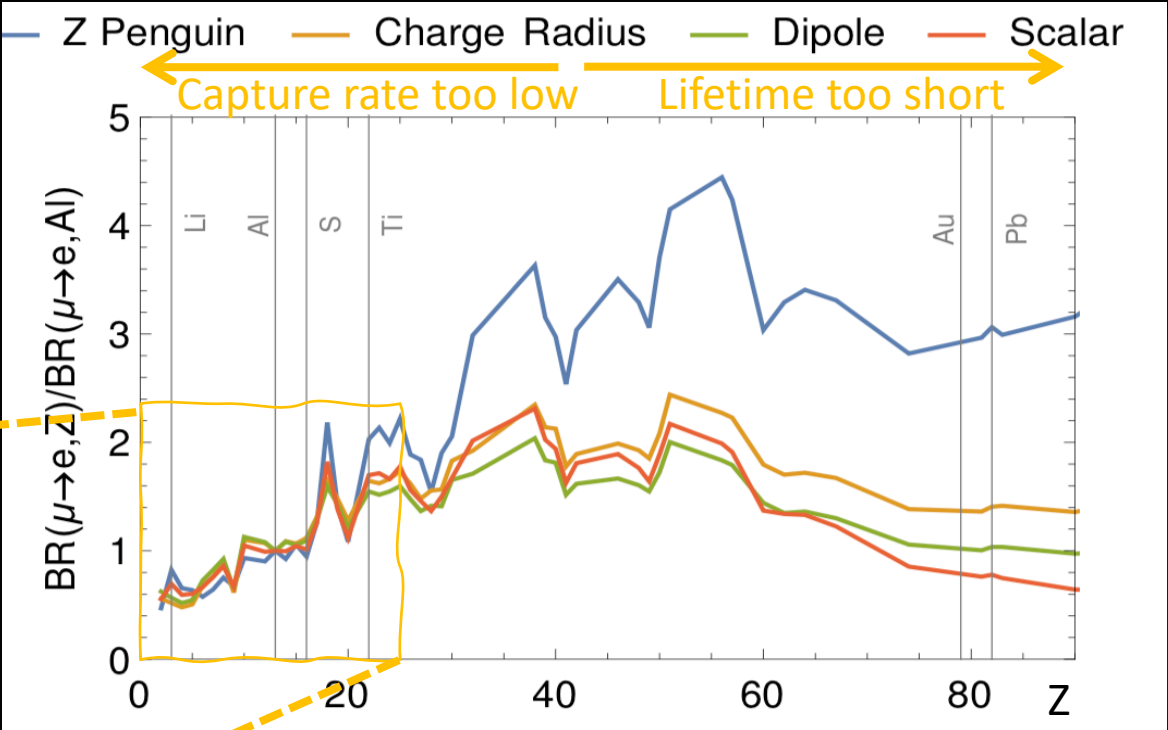
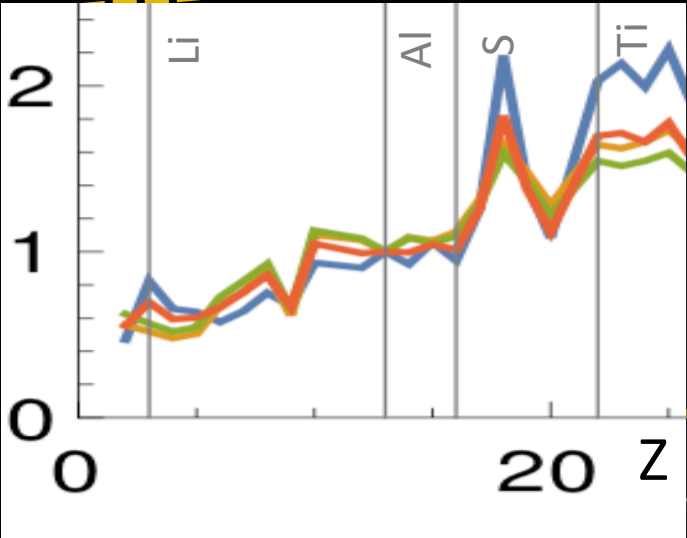
	S	D	V ¹	V ²
$\frac{B(\mu \rightarrow e, \text{Ti})}{B(\mu \rightarrow e, \text{Al})}$	$1.70 \pm 0.005_y$	1.55	1.65	2.0
$\frac{B(\mu \rightarrow e, \text{Pb})}{B(\mu \rightarrow e, \text{Al})}$	$0.69 \pm 0.02_{\rho_n}$	1.04	1.41	$2.67 \pm 0.06_{\rho_n}$

y = nuclear scalar form factor, ρ_n = nuclear neutron density

$$\text{BR}(\mu \rightarrow e) \propto |\text{DC}_{\text{DL}} + \text{S}^{\text{p}}\text{C}_{\text{S,L}}^{\text{p}} + \text{V}^{\text{p}}\text{C}_{\text{V,R}}^{\text{p}} + \text{S}^{\text{n}}\text{C}_{\text{S,L}}^{\text{n}} + \text{V}^{\text{n}}\text{C}_{\text{V,R}}^{\text{n}}|^2 + (\text{L} \leftrightarrow \text{R})$$

If we do see a signal in Al at Mu2e:

- Various operator coefficients add coherently in the amplitude.
 - Weighted by nucleus-dependent functions.
- Requires measurements of conversion rate in other target materials!
- Need to choose a target which is sensitive to directions Al is “blind” to



V. Cirigliano, S. Davidson, Y. Kuno, Phys. Lett. B 771 (2017) 242
 S. Davidson, Y. Kuno, A. Saporta, Eur. Phys. J. C78 (2018) 109
 Kitano et al 2002

Stopping Targets

Collaboration between theorist and experimentalists to understand best alternatives

Lithium:

- No detailed study, hard to contain, but not impossible.
- Weak signal, low discrimination power.
- (see Davidson et al 2019)

Aluminum:

- Single stable isotope
- Al(27) (spin 5/2)

Sulphur:

- Advantageous for e⁺ channel (see Beomki et al 2017)

Titanium:

- Multiple isotopes
- Ti(48) Ti(46)Ti(50) (spin-0) → no SD contribution
- Ti (47) (spin-5/2) or Ti(49)(spin-7/2) can measure SI contribution.

Vanadium:

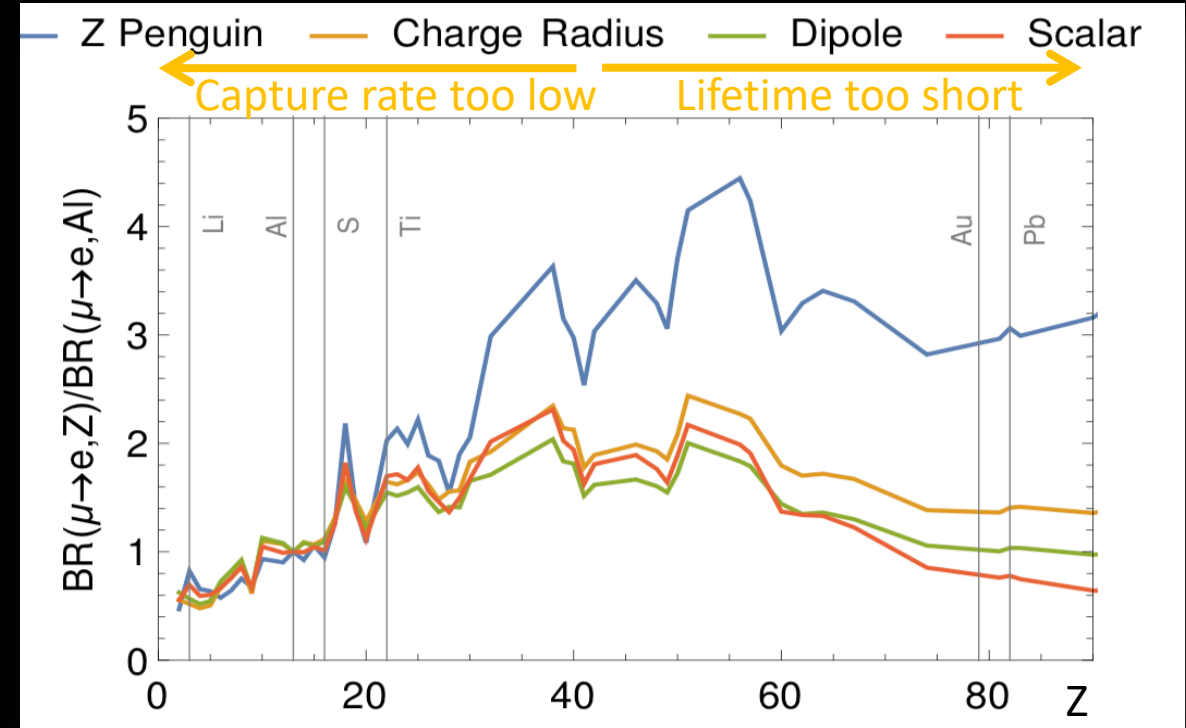
- Single isotope: V(51) makes up > 99% (spin-7/2)

Heavy Nuclei (Au or Pb):

- Strong discrimination.
- Short muon lifetime (increased pion backgrounds).
- Low sensitivity to spin-dependent contribution.

	S	D	V ¹	V ²
$\frac{B(\mu \rightarrow e, \text{Ti})}{B(\mu \rightarrow e, \text{Al})}$	$1.70 \pm 0.005_y$	1.55	1.65	2.0
$\frac{B(\mu \rightarrow e, \text{Pb})}{B(\mu \rightarrow e, \text{Al})}$	$0.69 \pm 0.02_{\rho_n}$	1.04	1.41	$2.67 \pm 0.06_{\rho_n}$

y = nuclear scalar form factor, ρ_n = nuclear neutron density

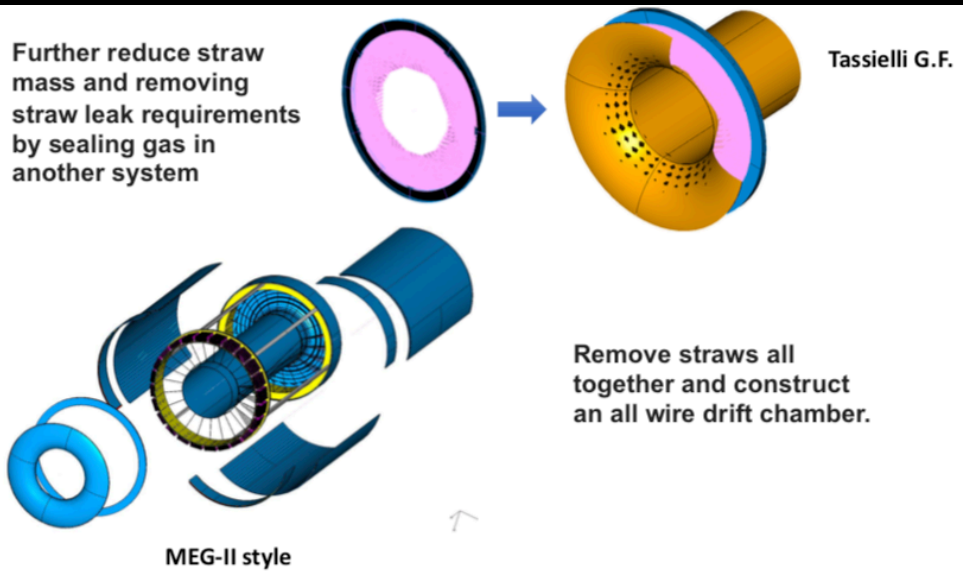
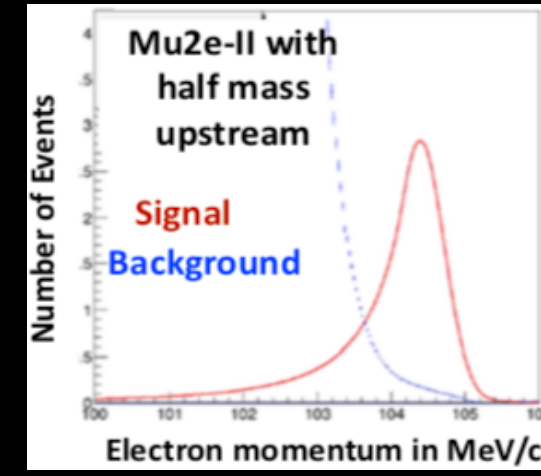
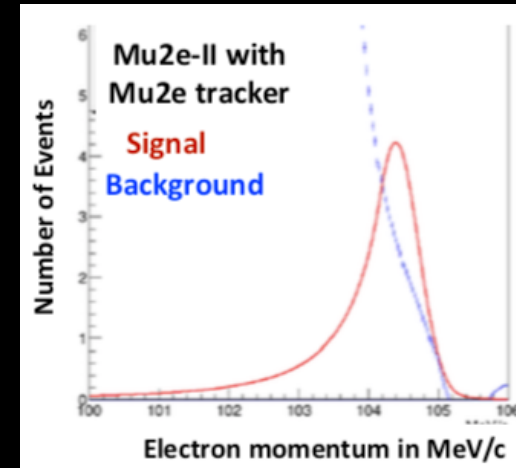
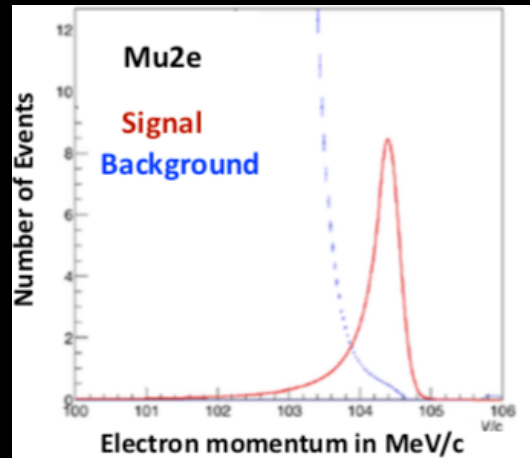


V. Cirigliano, S. Davidson, Y. Kuno, Phys. Lett. B 771 (2017) 242
 S. Davidson, Y. Kuno, A. Saporta, Eur. Phys. J. C 78 (2018) 109
 Kitano et al 2002

Tracker Requirements

DIO background would increase x10 in Mu2e-II.

Must improve momentum resolution to suppress DIO.



To meet Mu2e-II momentum resolution/background separation goals:

Reduce total Tracker Mass:

- Thinner straws ($8\mu\text{m}$)
- Remove the 200 angstrom gold layer from inside straw

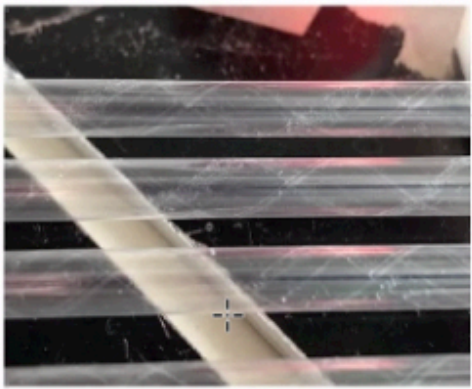
Change detector design:

- Use an ultra light gas vessel to ease straw leakage requirements
- Use different gas
- Consider all wires construction and remove the straws
- Or wires separated by mylar walls

Increased hit occupancy and timing window:

- 4x increase in PBI is estimated to reduce reconstruction efficiency by 30%.

Prototype Tracker Straws



Pressurized 8 μm Mylar Straws



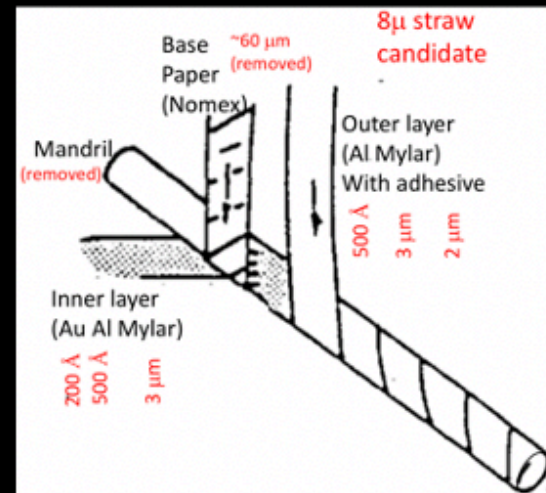
8 μm Mylar Straw

LDRD studying making thinner straws than Mu2e Issues being addressed Radiation levels would likely exceed the safety factor

- Expected 3 Mrad doses will damage some commercial off-the-shelf tracker components
- Consider using application-specific integrated circuit electronics to handle the radiation levels in the Mu2e-II environment

Discussed with vendor of straws and developed even thinner prototype:

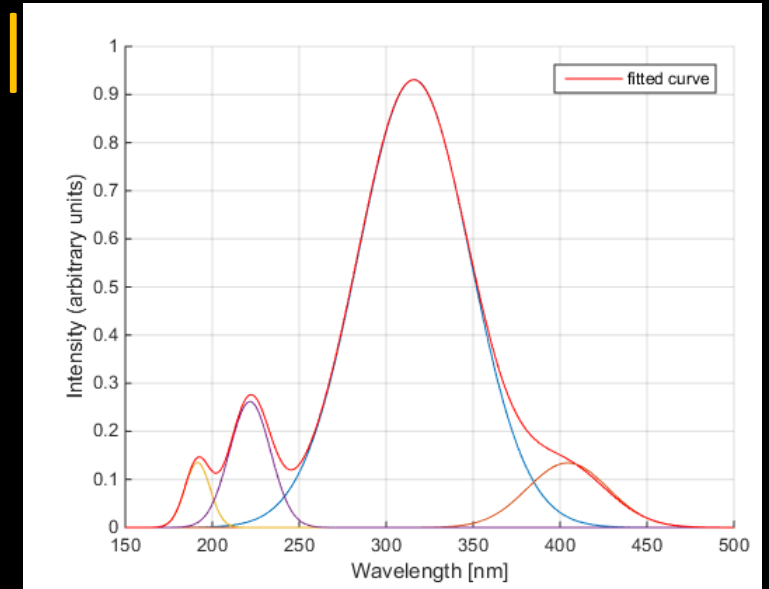
- Uses 3.5 μm Mylar + 1 μm adhesive + 3.5 μm Mylar double helical wrap = 8 μm
- Straws held at 15 PSI for multiple days and 400g Tension without visible distortion.



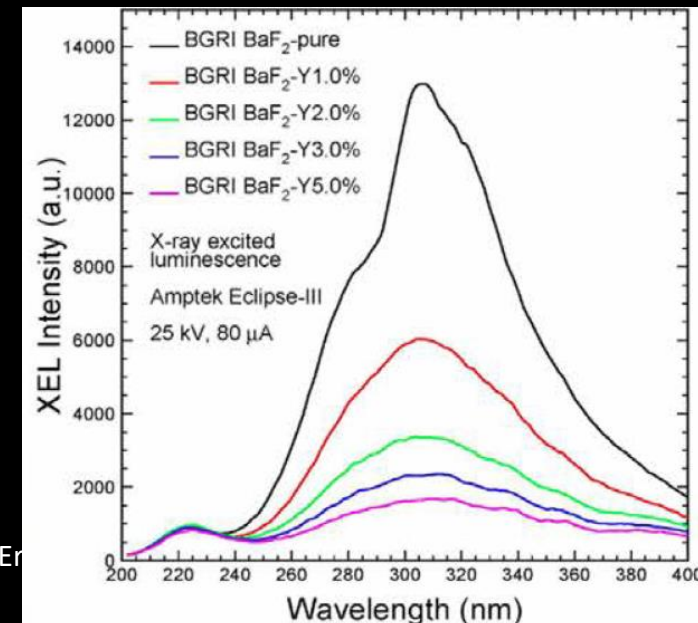
Barium Fluoride Calorimeter Crystal

- **Radiation doses and rates at Mu2e-II are high for CsI:**
 - Up to 900 krad and $1E13$ n [$1\text{MeVeq}/\text{cm}^2$]
- **BaF₂ is an excellent candidate for a fast, high rate, radiation-hard crystal for the Mu2e-II calorimeter:**
 - BaF₂ can survive up to 100 Mrad
- **Must have way of utilizing 220 nm fast component without interference from the larger 320 nm slow component.**
- **Slow suppression achieved by:**
 1. Rare Earth Doping (Y, La,Ce).
 2. Develop photo-detectors sensitive to UV only:
 - SiPM with an external filter
 - UV-sensitive photocathodes
 - Solar-blind MCP - SiPM “sees” only fast component.

R&D Collaboration between Caltech, JPL & FBK on-going

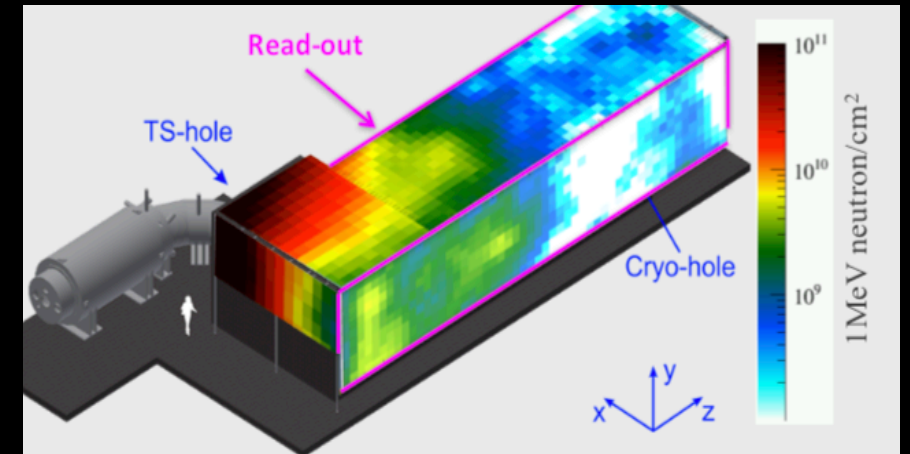
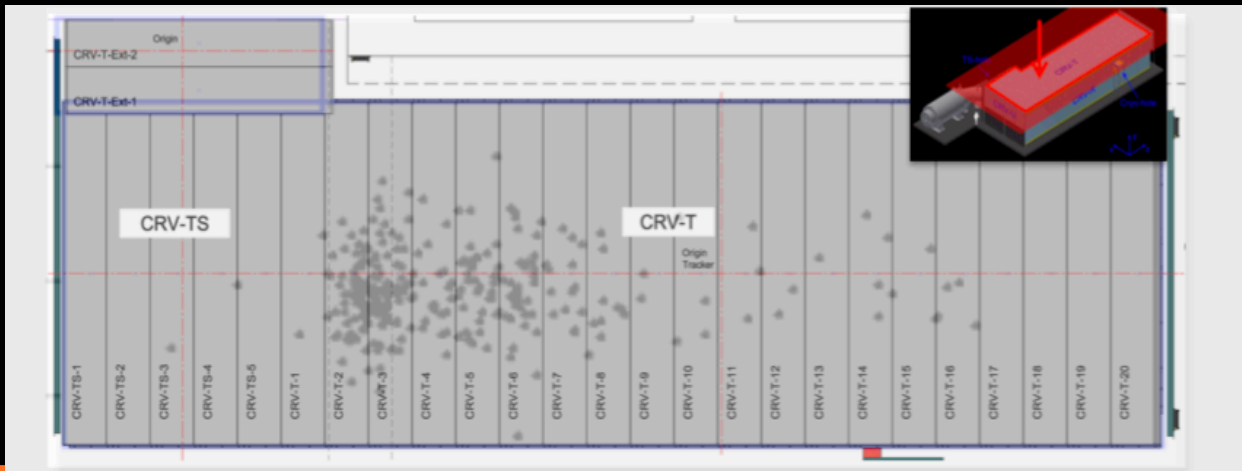


Actually two fast components ($t = 0.6$ ns) at 195 and 220 nm and two slow components ($t = 630$ ns) at 320 and 400 nm .



The Cosmic Ray Veto System (CRV)

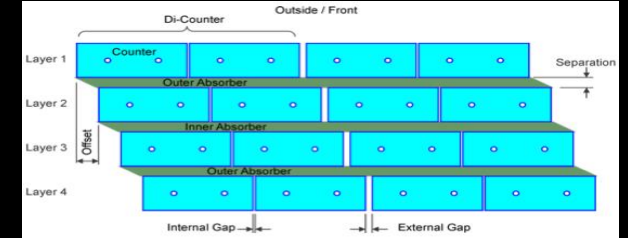
- **Expected live-time and therefore Cosmic Ray backgrounds will be 3 x higher for Mu2e-II**
 - Need to enhance the CRV performance in critical regions
 - **Light Yield degradation impacts CRV performance**
 - Must replace CRV
 - **Higher noise rates (x2-3) these impose challenges:**
 - Higher DAQ rates
 - Radiation damage
 - Induced dead-time
- Enhanced shielding, fine-granular layers, other technologies



The Cosmic Ray Veto System

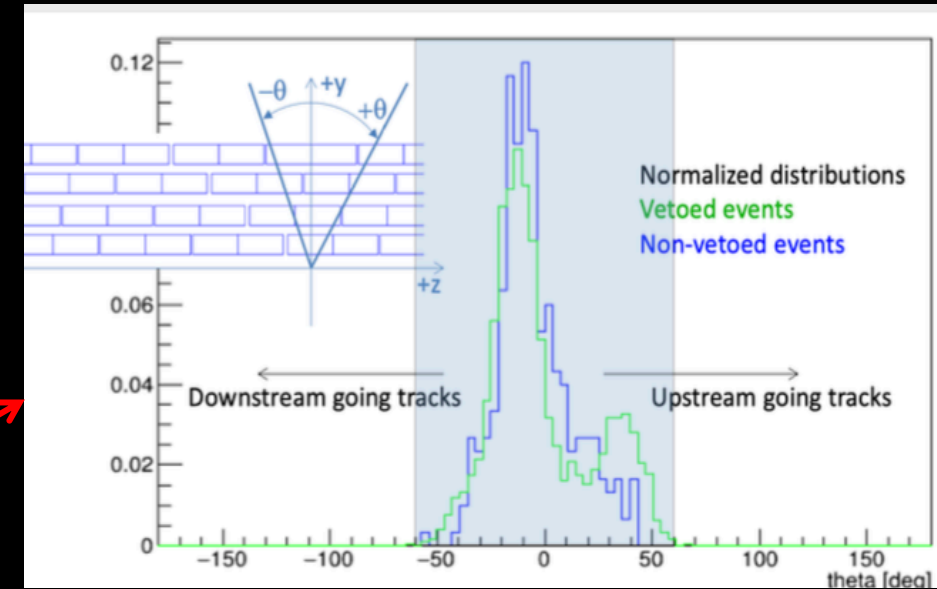
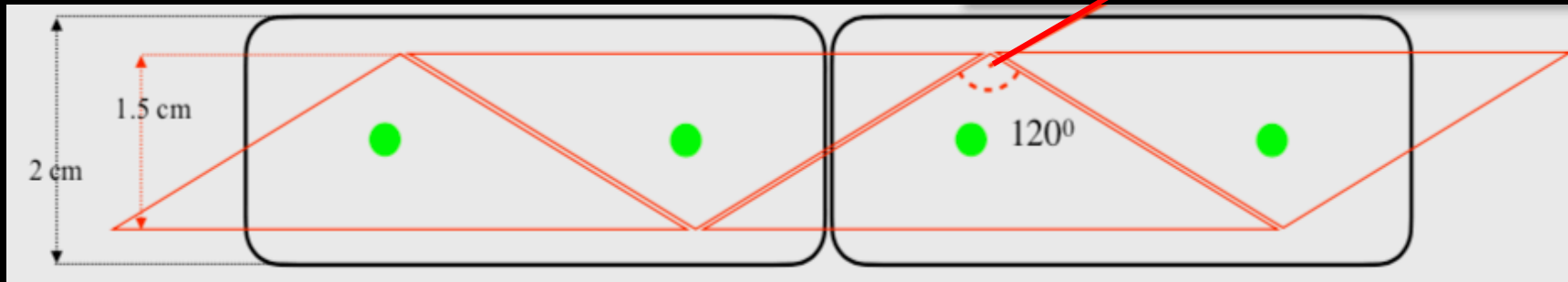


Mu2e Design: Rectangular Counters

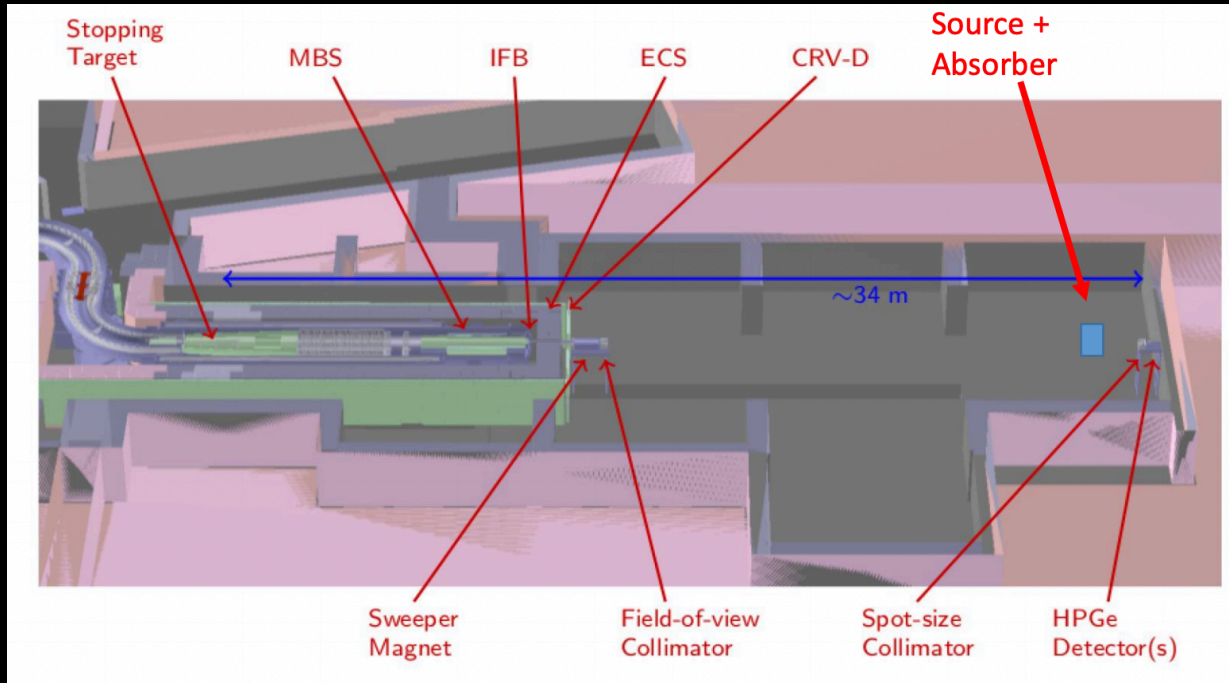


- Gaps between modules and counters and modules impact the CRV performance:
 - Reduce Gaps
 - Change geometry
 - Extra Layers
- **Triangular Bars:**
 - Improved efficiency due to reduced gaps
 - Lower dead time
 - Lower rate per channel
 - Simple design

Possible Mu2e-II Design



Stopping Target Monitor



STM measures the stopping muon rate at 10% precision over an hour period:

- **HPGe:** solid-state photon detector has a resolution of 1-2 keV
- **LaBr₃** : crystal has high rate capability and excellent radiation hardness

The Mu2e-II environment poses significant challenges for the HPGe detector:

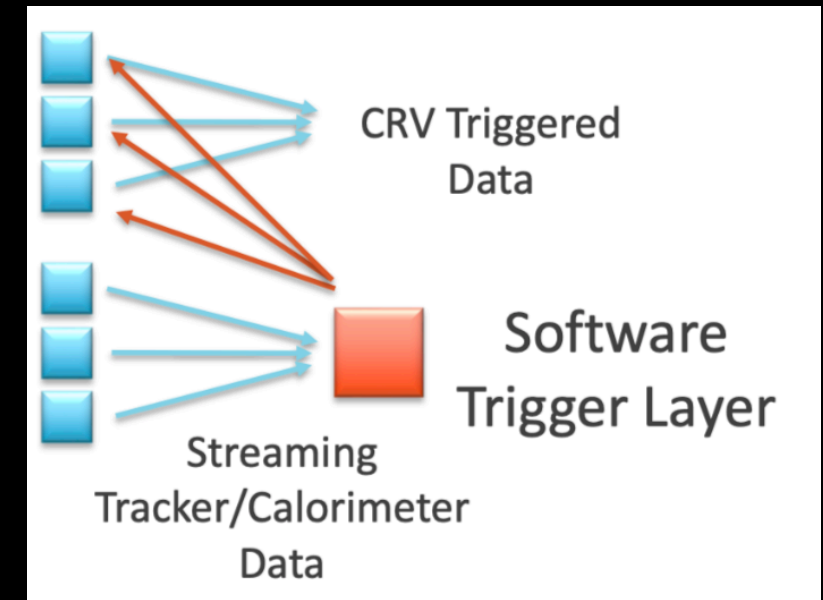
- The more intense prompt beam induced flash with the slow recovery time
- The higher levels of neutron damage

Mitigation strategies:

- Reduce the beam flash by increasing the absorber thickness at the cost of signal rate,
- Use the LaBr₃ and calibrate with the HPGe during special low intensity runs,
- Move STM off-axis - space may be an issue here,
- Replace some crystals in the calorimeter with LYSO or LaBr₃,
- Create a tertiary photon beam .

Trigger & Data Acquisition (TDAQ)

- **Increased data rate, more background and more detector channels:**
 - 10x data rate
 - X3 event size
 - 3000:1 rejection is needed to arrive at 14PB/year
- **Considerations:**
 - Reduced off-spill time to readout large front-end buffers
 - Streaming .v. triggered data taking
 - Radiation tolerances requirements
- **No large buffers for the CRV:**
 - Large CRV buffers + software trigger
 - Small CRV buffers + hardware trigger
- **Solutions:**
 - 2-level TDAQ based on FPGA pre-processing and trigger primitives
 - 2-level TDAQ system based on FPGA pre-filtering
 - TDAQ based on GPU co-processor
 - Trigger-less TDAQ based on software trigger.



Mu2e-II Resources

To stay upto date with everything Mu2e-II:

- **Public wiki page:**
 - <https://mu2eiiwiki.fnal.gov>
- **Learn about Mu2e-II:**
 - https://mu2eiiwiki.fnal.gov/wiki/Learn_about_Mu2e-II

We hold regular workshops – contact Frank Porter (fcpc@caltech.edu) for more information

Summary

- Mu2e-II is a proposed upgrade to Mu2e. Compelling physics case in either Mu2e scenario.
- Will push sensitivity down by at least $\times 10$ (SES $O(10^{-18})$).
- Plan to utilize Mu2e resources, including hardware, as much as possible, but the PIP-II environment is unique, and several components need redesign.
- Many studies underway to understand how to optimize all aspects of the experiment.
- Mu2e-II has a support from muon physics community and Fermilab's PAC
- Broad R&D program has been identified
- If approved, Mu2e-II expects to start data taking at the end of the decade
- For Snowmass 2022:
 - Plan to finalize studies by late winter 2021.
 - Snowmass White Paper due March 2022.

Thank You for Listening, any questions?

Useful Resources

1. S. T. Petcov, Sov. J. Nucl. Phys. **25**, 340 (1977); Yad. Fiz. **25**, 1336 (1977) [erratum].
2. S. M. Bilenky, S. T. Petcov, and B. Pontecorvo, Phys. Lett. B **67**, 309 (1977).
3. W. J. Marciano and A. I. Sanda, Phys. Lett. B **67**, 303 (1977).
4. B. W. Lee, S. Pakvasa, R. E. Shrock, and H. Sugawara, Phys. Rev. Lett. **38**, 937 (1977); **38**, 1230 (1977) [erratum] & Phys Rev D 16 5 1977
5. J. Adam *et al.* (EG Collaboration), Phys. Rev. Lett. **110**, 20 (2013).
6. W. Bertl *et al.* (SINDRUM-II Collaboration), Eur. Phys. J. **C47**, 337 (2006).
7. U. Bellgardt *et al.*, (SINDRUM Collaboration), Nucl. Phys. **B299**, 1 (1988).
8. A.M. Baldini *et al.*, “MEG Upgrade Proposal”, arXiv:1301.7225v2 [physics.ins- det].
9. Y. Kuno *et al.*, “COMET Proposal” (2007)
10. Mu2e TDR, arXiv:1501.05241
11. Nuclear Physics B - Proceedings Supplements Volumes 248–250, March–May 2014, Pages 35-4
12. A. Czarnecki *et al.*, “Muon decay in orbit: Spectrum of high-energy electrons,” Phys. Rev. D 84 (Jul, 2011) .
13. Sindrum-II “Improved limit of Branching Fraction of $\mu^- \rightarrow e^+$ in Titanium”, Phys Lett B 422 (1998) 334-338 (1998)

Charged Lepton Flavour Violation (CLFV)

- There are many well-motivated BSM theories which invoke CLFV mediated by (pseudo) scalar, (axial) vector, or tensor currents at rates close to current experimental limits i.e. $B \approx 10^{-15} - 10^{-17}$.
- A few examples:
 1. **SO(10) SUSY**
L. Calibbi *et al.*, Phys. Rev. D **74**, 116002 (2006), L. Calibbi *et al.*, JHEP **1211**, 40 (2012).
 2. **Scalar Leptoquarks**
J.M. Arnold *et al.*, Phys. Rev D **88**, 035009 (2013).
 3. **Different neutrino mass-generating Lagrangians lead to very different rates for CLFV**
Nuclear Physics B (Proc. Suppl.) 248–250 (2014) 13–19
 4. **Extended Higgs/Gauge sector**
 - **Left-Right Symmetric Models** C.-H. Lee *et al.*, Phys. Rev D **88**, 093010 (2013).
 - **Littlest Higgs** Monika Blanke, Andrzej J. Buras, Bjoern Duling, Stefan Recksiegel, Cecilia , Tarantino, Acta Phys.Polon.B41:657, 2010, arXiv:0906.5454v2 [hep-ph]

++

Detailed review: Lorenzo Calibbi, Giovanni Signorelli
arXiv:1709.00294 (2018)

Complementarity

Taken from: arXiv:0909.1333[hep-ph]

	AC	RVV2	AKM	δ LL	FBMSSM	LHT	RS
$D^0 - \bar{D}^0$	★★★★	★	★	★	★	★★★★	?
ϵ_K	★	★★★★	★★★★	★	★	★★	★★★★
$S_{\psi\phi}$	★★★★	★★★★	★★★★	★	★	★★★★	★★★★
$S_{\phi K_S}$	★★★★	★★	★	★★★★	★★★★	★	?
$A_{CP}(B \rightarrow X_s \gamma)$	★	★	★	★★★★	★★★★	★	?
$A_{7,8}(B \rightarrow K^* \mu^+ \mu^-)$	★	★	★	★★★★	★★★★	★★	?
$A_9(B \rightarrow K^* \mu^+ \mu^-)$	★	★	★	★	★	★	?
$B \rightarrow K^{(*)} \nu \bar{\nu}$	★	★	★	★	★	★	★
$B_s \rightarrow \mu^+ \mu^-$	★★★★	★★★★	★★★★	★★★★	★★★★	★	★
$K^+ \rightarrow \pi^+ \nu \bar{\nu}$	★	★	★	★	★	★★★★	★★★★
$K_L \rightarrow \pi^0 \nu \bar{\nu}$	★	★	★	★	★	★★★★	★★★★
$\mu \rightarrow e \gamma$	★★★★	★★★★	★★★★	★★★★	★★★★	★★★★	★★★★
$\tau \rightarrow \mu \gamma$	★★★★	★★★★	★	★★★★	★★★★	★★★★	★★★★
$\mu + N \rightarrow e + N$	★★★★	★★★★	★★★★	★★★★	★★★★	★★★★	★★★★

★★★★ = Discovery Sensitivity

Table 8: “DNA” of flavour physics effects for the most interesting observables in a selection of SUSY and non-SUSY models ★★★★★ signals large effects, ★★ visible but small effects and ★ implies that the given model does not predict sizable effects in that observable.

Discovery sensitivity across the board.
Relative Rates however will be model dependent.

Model	$\mu \rightarrow eee$	$\mu N \rightarrow eN$	$\frac{\text{BR}(\mu \rightarrow eee)}{\text{BR}(\mu \rightarrow e \gamma)}$	$\frac{\text{CR}(\mu N \rightarrow eN)}{\text{BR}(\mu \rightarrow e \gamma)}$
MSSM	Loop	Loop	$\approx 6 \times 10^{-3}$	$10^{-3} - 10^{-2}$
Type-I seesaw	Loop*	Loop*	$3 \times 10^{-3} - 0.3$	$0.1 - 10$
Type-II seesaw	Tree	Loop	$(0.1 - 3) \times 10^3$	$\mathcal{O}(10^{-2})$
Type-III seesaw	Tree	Tree	$\approx 10^3$	$\mathcal{O}(10^3)$
LFV Higgs	Loop [†]	Loop* [†]	$\approx 10^{-2}$	$\mathcal{O}(0.1)$
Composite Higgs	Loop*	Loop*	$0.05 - 0.5$	$2 - 20$

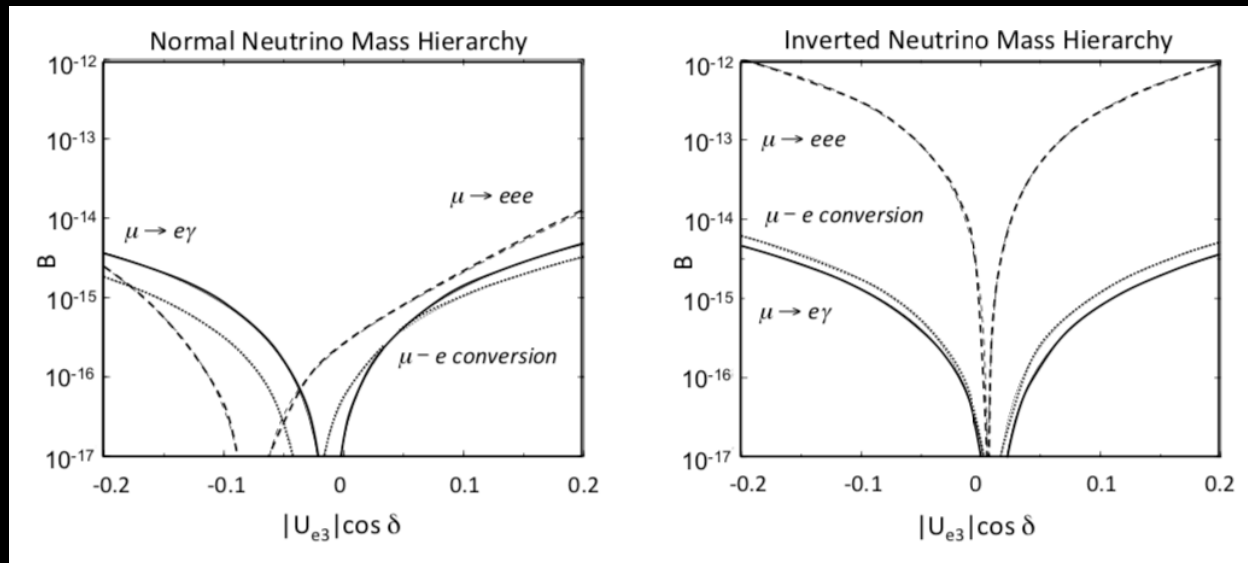
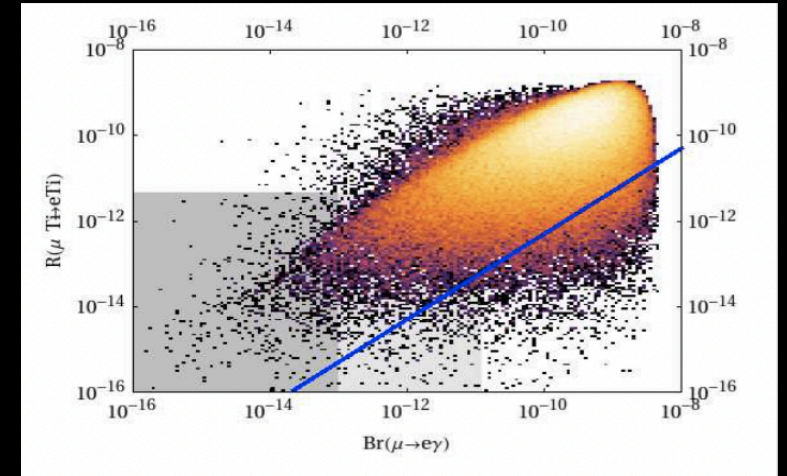
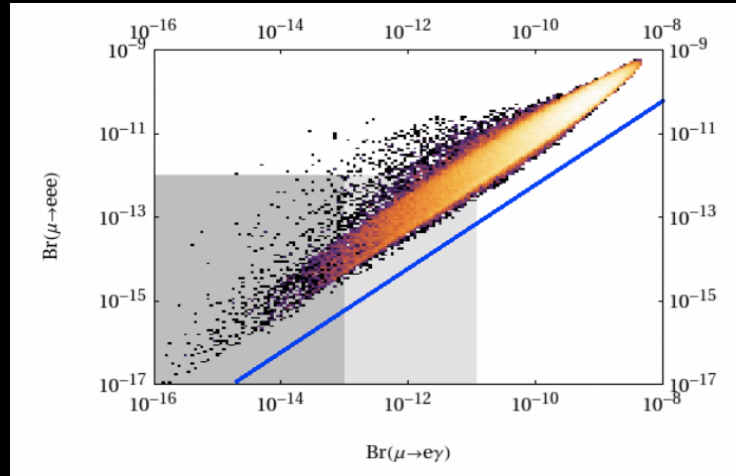
from L. Calibbi and G. Signorelli, Riv. Nuovo Cimento, 41 (2018) 71

arXiv:1709.00294v2[hep-ph]

BSM theories and CLFV Rates

“Littlest Higgs” (LHT) - Correlation between $\mu \rightarrow e\gamma$ and $\mu \rightarrow e$ conversion in Ti as obtained from a general scan over the LHT parameters. The solid blue line represents the dipole contribution to $R(\mu\text{Ti} \rightarrow e\text{Ti})$.

Blanke et al arXiv:0906.5454v2 [hep-ph]

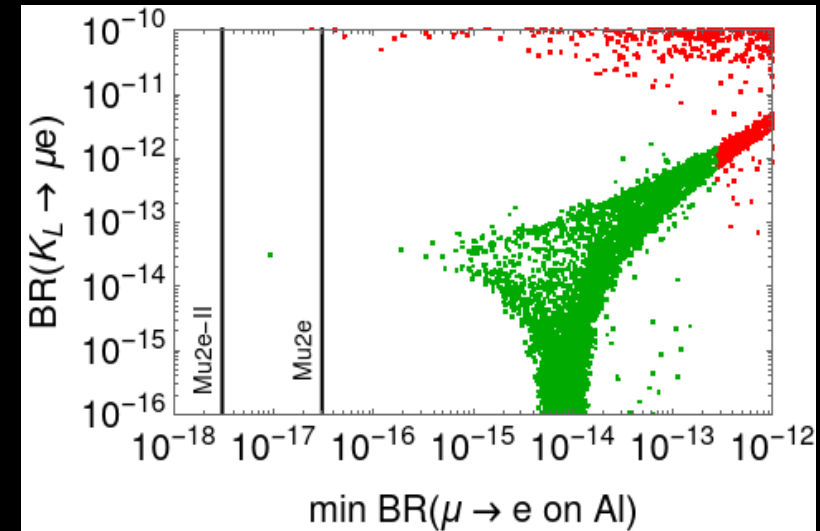
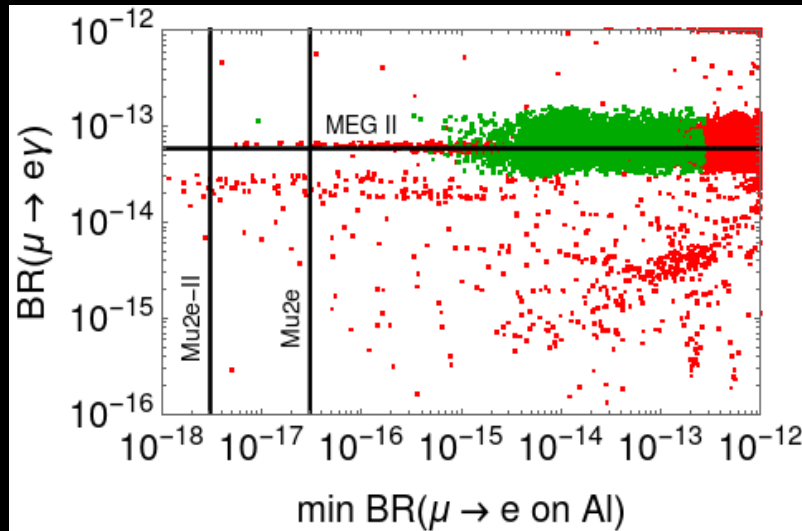


Neutrino Mass/ Extended Higgs - if neutrino Majorana masses are a consequence of the existence of SU(2) triplet Higgs fields.

Data from neutrino oscillation experiments, LHC experiments and CLFV should ultimately allow one to thoroughly test particular Higgs triplet models.
M. Kakizaki et al Phys. Lett. **B566**, 210 (2003).

Leptoquarks

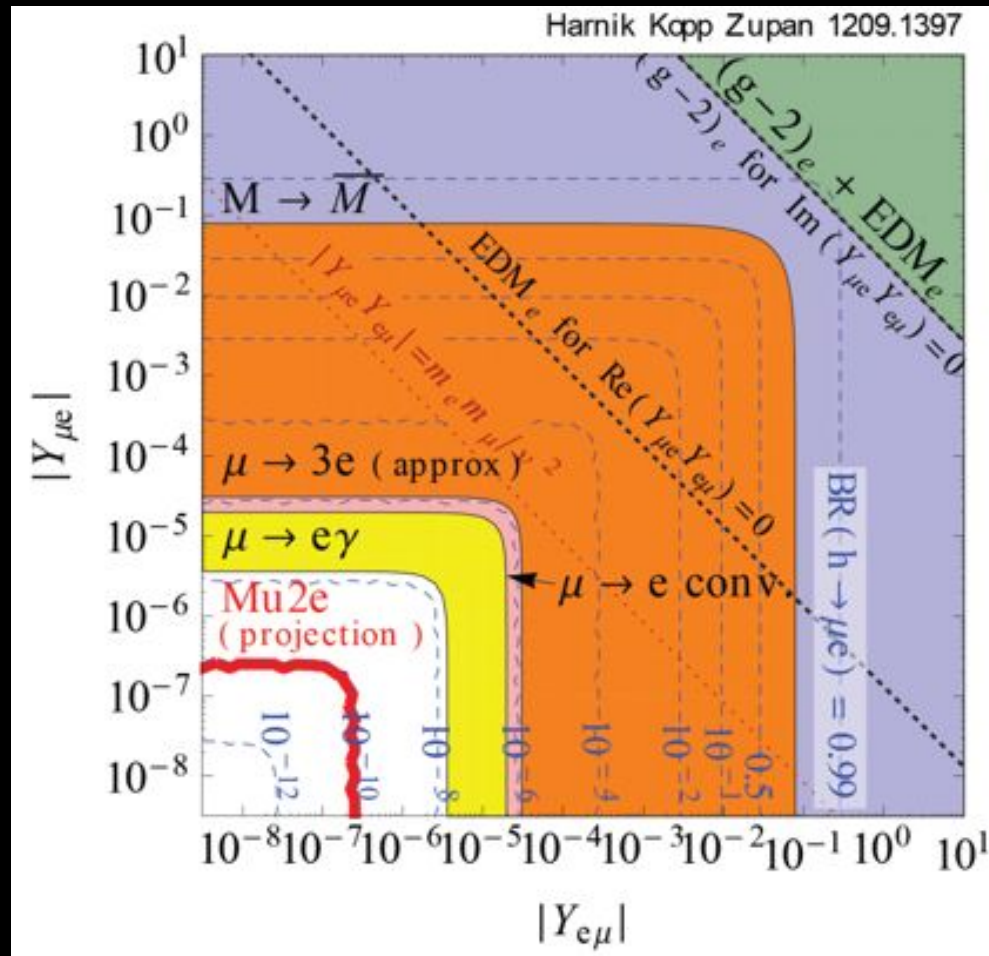
- Pati-Salam Leptoquarks: B-meson anomalies could be explained by two scalar leptoquarks, whose couplings enter neutrino masses as well. Type-II seesaw dominance is favored. [Heeck & Teresi, 1808.07492](#)



Plots: Julian Heck

- Flavor structure fixed by neutrino mass/mixing; scale Λ fixed to explain B-meson anomaly $R(K)$.
- Predicts testable rates in Mu2e!
- Explain B meson anomalies through adding 2 scalar leptoquarks: [Bigaran, Gargalionis, Volkas, 1906.01870](#) $\rightarrow B(\mu N \rightarrow e N) < 3 \times 10^{-13}$

Constraining Flavour Violating Higgs Decays



- Can also help constrain flavor violating Higgs decays [Harnik, J. Kopp and J. Zupan, JHEP 3, 26 \(2013\)](#).
- Higgs LFV decays arise in many frameworks of New Physics at the electroweak scale such as two Higgs doublet models, extra dimensions, or models of compositeness.
- Current $\mu \rightarrow e$ conversion implies:

$$\sqrt{|Y_{\mu e}|^2 + |Y_{e\mu}|^2} < 4.6 \times 10^{-5}$$

- Mu2e is expected to be sensitive to:

$$\sqrt{|Y_{\mu e}|^2 + |Y_{e\mu}|^2} > \text{few} \times 10^{-7}.$$

- Where $|Y_{\mu e}|$ and $|Y_{e\mu}|$ are flavor-violating Yukawa couplings for a 125 GeV Higgs boson i.e. $h \rightarrow \mu e$.
- Very strong limits on LFV Higgs decays for 1st-2nd generation**

Possibilities

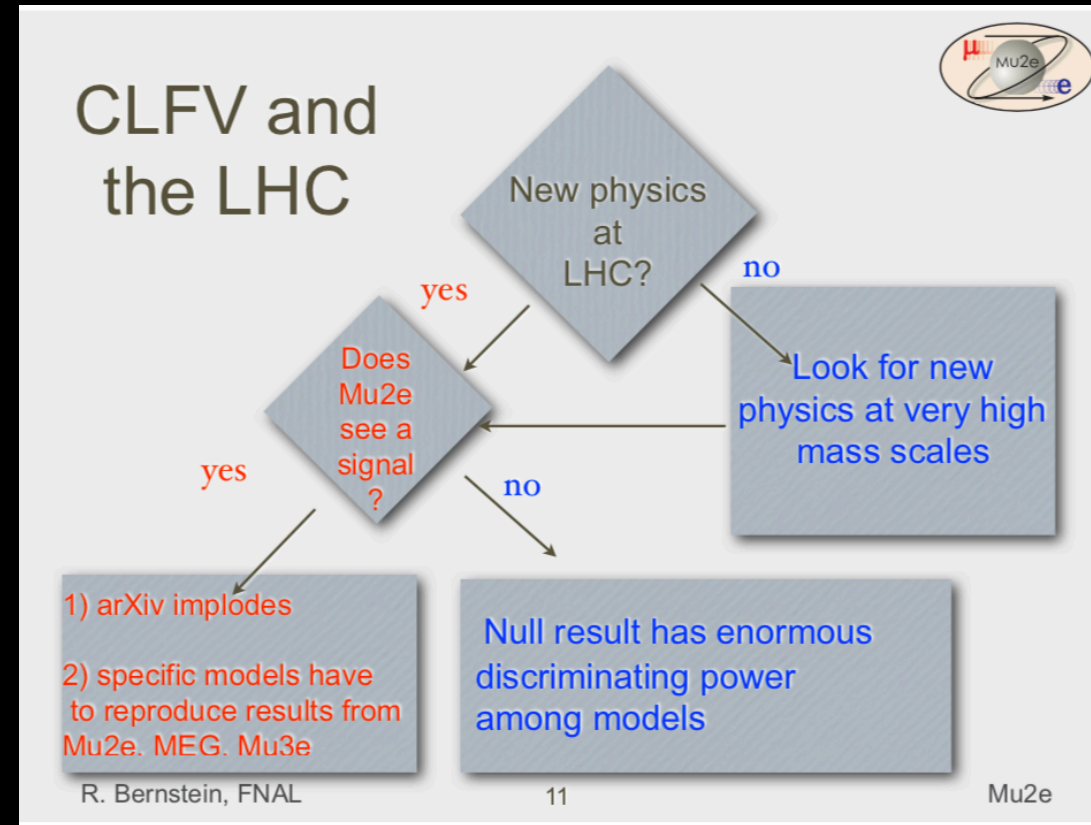
Over the coming decade:

- BSM searches and Higgs physics at the LHC/HL-LHC
- Neutrino mass hierarchy and CPV in neutrino sector

both are extended and complemented by muon-to-electron searches such as Mu2e:

If new physics is observed at the LHC, Mu2e etc. is critical to elucidating degenerate models.

If the new physics is at a higher scale then Mu2/3e can probe it

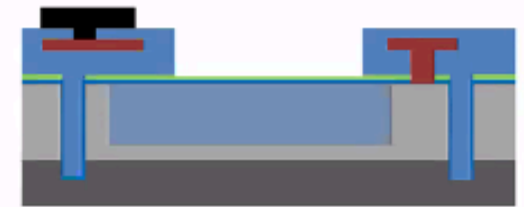


SiPM Fabrication

Increase number of layers to get better removal of slow component

SiPM fabrication and test

- FBK has fabricated wafers based on current NUV designs, with various modifications, including guard ring structures
- FBK thins or removes SiNx passivation layer
- ALD filters are deposited at JPL
- The wafers are returned to FBK for probing and dicing into chips
- 6x6mm devices with three-layer filters have been fabricated and tested at Caltech
 - Filter performance and PDE as a function of wavelength have been measured with a spectrophotometer down to 200nm
 - We have characterized excess noise performance
 - We have then taken radioactive decay and cosmic ray spectra with pure BaF₂ crystals, measuring the fast/slow scintillation yield



SiPM R&D

So far:

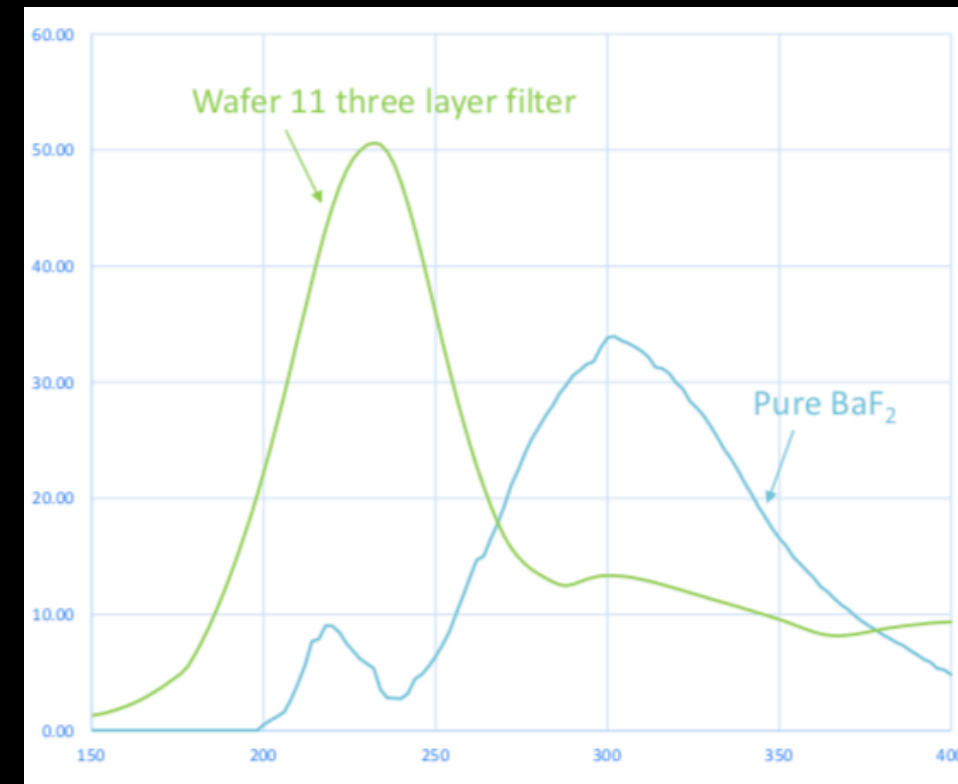
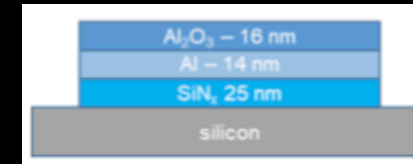
- Collaboration between Caltech, JPL and FBK
- Built three layer ALD filter on a 6x6 mm NUV SiPM structure, exploring different SiNx passivation layers, guard ring structures.
- Fabricated 2x3 arrays of the 6x6 mm chips, biased in series parallel configuration à la MEG and Mu2e to read out larger crystals

Results show:

- Began with a simple three-layer filter designed to incorporate a thinned SiNx passivation layer.

Next Step:

- Study 5 layer filter



Mu2e-II: 2020 Snowmass LOI

In August 2020 we submitted our main LOI with ~130 signatures.

There were several additional LOI's from sub-groups:

- Beam delivery for Mu2e-II
- Calorimeter
- Cosmic Ray Veto
- Production target
- Stopping target monitor
- Theory
- Tracker
- Trigger/DAQ, 2 level, FPGA, scheme A
- Trigger/DAQ, 2 level, FPGA, scheme B
- Trigger/DAQ, 2 level, GPU
- Trigger/DAQ, software trigger

Links here:

https://mu2eiiwiki.fnal.gov/wiki/Snowmass21_Information#LOIs

August 31, 2020

Mu2e-II

Letter of Interest for Snowmass 2021

K. Byrum,¹ Y. Oksuzian,¹ P. Winter,¹ J. Miller,² N. H. Tran,² J. Mott,³ D. Denisov,⁴ W. J. Marciano,⁴
R. Bonventre,⁵ D. N. Brown,⁵ A. W. J. Edmonds,⁵ Yu. G. Kolomensky,^{ab,5} K. Harrig,⁶ E. Prebys,⁶
L. Borrel,⁷ B. Echenard,⁷ D. G. Hitlin,⁷ C. Hu,⁷ D. X. Lin,⁷ S. Middleton,⁷ J. Oyang,⁷ F. C. Porter,⁷
L. Zhang,⁷ R.-Y. Zhu,⁷ R. Szafron,⁸ K. Badgley,⁹ R. H. Bernstein,⁹ B. C. K. Casey,⁹ R. Culbertson,⁹
G. Drake,⁹ A. Gaponenko,⁹ H. D. Glass,⁹ D. Glenzinski,⁹ L. Goodenough,⁹ A. Hocker,⁹
M. Kargiantoulakis,⁹ B. Kiburg,⁹ R. K. Kutsche,⁹ P. A. Murat,⁹ D. Neuffer,⁹ V. S. Pronskikh,⁹
G. Rakness,⁹ R. A. Rivera,⁹ D. Stratakis,⁹ T. Strauss,⁹ R. Tschirhart,⁹ J. Whitmore,⁹ M. Yucel,⁹
C. Bloise,¹⁰ E. Diociaiuti,¹⁰ R. Donghia,¹⁰ S. Giovannella,¹⁰ F. Happacher,¹⁰ S. Miscetti,¹⁰
I. Sarra,¹⁰ M. Martini,¹¹ A. Ferrari,¹² S. E. Mueller,¹² R. Rachamin,¹² E. Barlas-Yucel,¹³
S. Ganguly,¹³ S. P. Denisov,¹⁴ V. Evdokimov,¹⁴ A. V. Kozelov,¹⁴ A. V. Popov,¹⁴ I. A. Vasilyev,¹⁴
I. Bailey,¹⁵ F. Grancagnolo,¹⁶ G. Tassielli,¹⁶ T. Teubner,¹⁷ R. T. Chislett,¹⁸ G. G. Hesketh,¹⁸
D. N. Brown,¹⁹ M. Lancaster,²⁰ M. Campbell,²¹ D. Ambrose,²² K. Heller,²² J. D. Crnkovic,²³
M. A. C. Cummings,²⁴ L. Calibbi,²⁵ M. J. Syphers,²⁶ C. Kampa,²⁷ M. MacKenzie,²⁷ S. Donati,²⁸
C. Ferrari,²⁸ A. Gioiosa,²⁸ V. Giusti,²⁸ L. Morecalchi,²⁸ D. Pasciuto,²⁸ E. Pedreschi,²⁸
F. Spinella,²⁸ S. Di Falco,²⁸ M. T. Hedges,²⁹ M. Jones,²⁹ J.-F. Caron,³⁰ C. J. Han,³¹ Y. Wang,³¹
Z. Y. You,³¹ A. M. Zanetti,³² E. V. Valetov,³³ E. C. Dukes,³⁴ R. Ehrlich,³⁴ R. C. Group,³⁴
J. Heeck,³⁴ P. Q. Hung,³⁴ S. M. Demers,³⁵ G. Pezzullo,³⁵ K. R. Lynch,³⁶ and J. L. Popp³⁶

¹Argonne National Laboratory, Lemont, Illinois 60439, USA

²Boston University, Boston, Massachusetts 02215, USA

³Boston University, Boston, Massachusetts 02215, USA; Fermi National Accelerator Laboratory, Batavia, Illinois 60510, USA

⁴Brookhaven National Laboratory, Upton, New York 11973 USA

⁵University of California^a, Lawrence Berkeley National Laboratory^b, Berkeley, California 94720, USA

⁶University of California, Davis, California 95616, USA

⁷California Institute of Technology, Pasadena, California 91125, USA

⁸CERN TH CH-1211 Geneva 23, Switzerland

⁹Fermi National Accelerator Laboratory, Batavia, Illinois 60510, USA

¹⁰Laboratori Nazionali di Frascati dell'INFN, I-00044 Frascati, Italy

¹¹Laboratori Nazionali di Frascati dell'INFN, I-00044 Frascati, Italy; Università degli Studi Guglielmo Marconi, 00193, Rome, Italy

¹²Helmholtz-Zentrum Dresden-Rossendorf, Dresden 01328, Germany

¹³University of Illinois at Urbana-Champaign, Urbana, Illinois 61801, USA

¹⁴NRC Kurchatov Institute, IHEP, 142281, Protvino, Moscow region, Russia